X rays from *z*-pinches on relativistic electron-beam generators

N. R. Pereira
Berkeley Research Associates, Inc., P. O. Box 852, Springfield, Virginia 22150
J. Davis
Plasma Physics Division, Naval Research Laboratory, Washington, DC 20375-5000

This review summarizes recent experimental data on imploding *z*-pinches and their radiation output, and gives an overview of theoretical issues concerning radiation production in the pinch plasma. A *z*-pinch plasma is created when the current from a fast, powerful electrical generator compresses and heats a small amount of material between the electrodes. The hot, dense plasma emits copious amounts of radiation extending from the visible to the x-ray region. With a 10-TW electrical discharge the radiative power may be a few TW, with an energy per pulse of up to tens of kilojoules. Our interest is mainly in the photons with energy around 1 keV, which are useful in x-ray lithography, microscopy, surface studies, and other applications.

TABLE OF CONTENTS

I. INTRODUCTION

The bluish light flash signaling the demise of the filament in a light bulb is produced by about 100 W of household power. X-ray producing *z*-pinches are high-power versions of blowing up filaments. The electrical power input reaches 1 TW (10^{12} W) or even higher, with currents measured in megaamperes (MA) and voltages in megavolts (MV). The current's magnetic pressure along the cylindrical axis of symmetry between two electrodes compresses the filament, hence the name *z*-pinch.

The temperature in a light bulb filament is about 3000 K or ~ 0.3 eV. On increasing the power input the filament temperature should increase: assuming a (temperature)^4 relation like that of a blackbody radiator, an increase in power by a factor 10^{10} extrapolates to a temperature on the order of $0.3\ \text{eV} \times (10^{10})^{1/4} \approx 100$ eV; temperatures in this range are indeed obtained in *z*-pinches. The high power can be sustained only during a short time, perhaps 100 ns.

A hot, dense plasma can be created by exploding a single wire, but multiple parallel wires offer better energy efficiency. The parallel currents in the wires attract each other and the wires accelerate toward the center, storing electrical energy as kinetic energy of implosion. The kinetic energy is thermalized in the collision of the oppositely directed wires, resulting in a hot, dense plasma on axis. The plasma energy from the implosion is augmented by joule heating during implosion, which ionizes wires, and by continued heating during stagnation. The same effect is obtained by smearing out the wire mass in a hollow cylindrical shell.

Imploding *z*-pinches are efficient x-ray producers. Typically more than 50% of the plasma energy appears as sub-keV radiation. Perhaps about 10% is radiated in soft x rays between 1 and 10 keV, usually from localized "bright spots." Sometimes minor amounts of high-energy bremsstrahlung are generated, typically less than 1%. The remaining energy goes into magnetic field energy of the vacuum surrounding the pinch and into the thermal energy of the plasma; this energy appears as kinetic energy of the expanding plasma, i.e., the explosion of the pinch after the radiation pulse.

This review discusses the imploding *z*-pinch for its use as an x-ray source. We emphasize imploding plasmas because in the United States this configuration is the most common. Early examples are the hollow cylinder proposed by Turchi (1973), the multiple wires (Stallings, 1976), and a cylindrical or annular gas shell (Shiloh, 1978). Single exploding wires are mentioned where appropriate. For typical early results on exploding wires see Mosher (1973, 1975). Much work on single wires is continuing in the Soviet Union, see e.g., Zakharov (1983), Baksht (1983, 1987), or Aranchuk (1986).

Not reviewed here is the imploding liner research on the large capacitor bank at AFWL, which is well documented in a series of papers (Baker, 1978; Degnan, 1981; Roderick, 1983). Another summary is the *z*-pinch work at Imperial

 0021-8979/88/1500R1-27$02.40

College (Dangor, 1986). Much lower-temperature ($\sim$1 eV) VUV emitting pinches were extensively reviewed by Finken (1983). Not related to x rays are applications of *z*-pinches for the generation of large magnetic fields (e.g., Felber, 1985; Wessel, 1986), and as a focusing device in high-energy particle accelerators (e.g., Dothan, 1987). Quite related but still omitted is the use of *z*-pinches for x-ray laser research (for a review, see Davis, 1988), and the hydrogen *z*-pinch for thermonuclear fusion. This approach to fusion is discussed by Haines (1982): for recent experimental results see Sethian (1987), and for a review of neutron production mechanisms see Vikhrev (1987) and Trubnikov (1987). A complete bibliography on *z*-pinch fusion is available from Robson (1987).

Peripheral topics of interest are the pulse power technology needed for driving the pinch (see Camarcat, 1985) and x-ray diagnostic techniques: for quantitative aspects see e.g., Kühne (1985), Eidmann (1986b), and especially Henke (1984a, 1984b).

X-ray sources similar to the *z*-pinches are vacuum sparks, the plasma focus, and laser-produced plasmas. Although they fall outside this review their x-ray characteristics are sufficiently similar to the *z*-pinches to merit explicit mention.

In a vacuum spark the current that is passed through an extremely small amount of material that is blown off an electrode, either spontaneously or in a controlled manner with a laser. This gives a hot but perhaps nonthermal plasma with "temperature" of 1–30 keV at various times during the pulse. The x rays come out in multiple bursts (e.g., Burhenn, 1984; Seeley, 1984; Negus, 1979; Cilliers, 1975; Lee, 1975/1974/1971). Vacuum sparks were reviewed by Korop (1979) and by Negus (1979).

In a plasma focus the discharge must find its own path through an initially homogeneous gas fill, leading to a somewhat erratic pinch. The *z*-pinch configuration, wherein the current can only go where sufficient material is deliberately introduced, makes the discharge more reproducible. Most plasma focus work is directed toward thermonuclear fusion or pulsed neutron production, not to efficient x-ray generation.

Plasmas are created in the focus of optical lasers, with a typical fluence around 100 TW/cm^2. The plasma may reach a temperature in the neighborhood of 1 keV (e.g., Glibert, 1980; Nicolosi, 1981; Pepin, 1985; Gerritsen, 1986; Mochizuki, 1986; Eidmann, 1986a; Kodama, 1986; Phillion, 1986). The x-ray output per pulse is usually modest, even with a high ($\sim$50%) conversion efficiency from optical light to XUV and soft x rays. The world's largest laser, Nova at LLNL (Campbell, 1986), produces up to $\sim$100 kJ/pulse in the optical, and should yield comparably impressive x-ray pulses. A laser-produced plasma is particularly convenient in many applications because the pulse power is far away from the plasma, while in other applications the potential rep-rate capability of the laser is important (see, e.g., Nagel, 1984; Michette, 1986: also small conventional bremsstrahlung sources can be repetitively pulsed, see, e.g., Davanloo, 1987).

A completely different x-ray source is synchrotron radiation, generated by wiggling GeV electrons. The electrons are accelerated in bunches, and as a consequence the radiation comes out in a continuous train of polarized XUV or soft x-ray bursts with low instantaneous but high average power (see, e.g., Winick, 1980; Koch, 1983; Attwood, 1985; Brown, 1986). The special qualities of these x rays come at a price: a large multiuser facility may cost on the order of \$100M. In contrast, a small *z*-pinch that produces 10 J/shot of incoherent keV-like x rays costs perhaps $\sim$\$100 000, and the hardware fits in a laboratory corner.

Figure 1 summarizes the parameter regime of the output generated with the various techniques. The *z*-pinch operates in the 1–10 TW regime with a plasma temperature of 0.1–1 keV. The total energy per pulse depends on the desired photon energy, and obviously on the machine size. Figure 1 suggests a typical power range for neon and argon gas puffs, where $\sim$50% of the photons come out in a single or at most a few narrow lines. Photon energies in between come from elements with intermediate atomic number, or in broadband radiation from higher atomic number elements such as nickel. Laser-produced plasmas (LPP) provide less power at comparable photon energies, and vacuum sparks much less power but in more energetic photons. The x rays are incoherent, and the average power is typically low because most are single-shot devices. Laser-driven x-ray lasers promise a short high-power burst of coherent photons with energy below $\sim$100 eV, but not more energy per pulse (right scale).

The lasers on the left-hand side attain enormous powers in coherent light close to the visible, below at most $h\nu \sim 5$ eV; frequency multiplication can give higher photon energies at rapidly decreasing powers. Synchrotron-produced photons are available over a wide energy region, but as always with decreasing power the higher the photon energy.

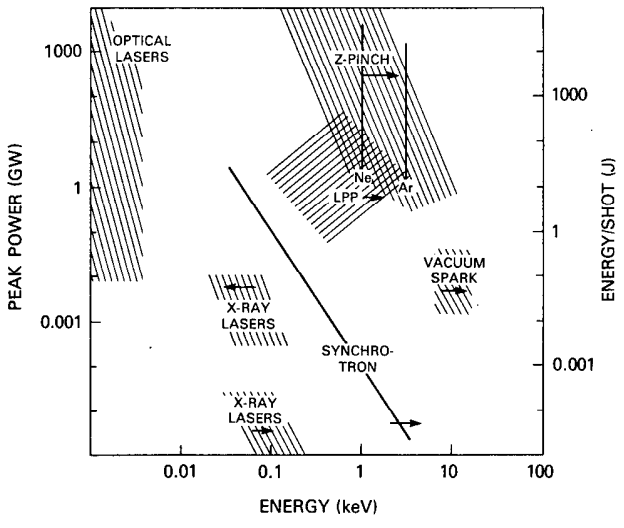

FIG. 1. Typical peak power and energy per shot for the *z*-pinch, laser-produced plasma (LPP), and vacuum spark x-ray sources as function of a typical photon energy; the vertical lines are the photon energies for the *K* lines of neon and argon. Sources of coherent x rays are the x-ray lasers, whose very short pulse length is reflected in the relatively high peak power. Synchrotron radiation consists of short pulses at high repetition rates, with average power (in watts) on the right scale. Optical lasers are shown for comparison (upper left).

A final note: our references are almost exclusively limited to the archival literature over the last decade. This choice is most helpful to the reader, while still representative of the available data. We apologize to our colleagues whose work is inadequately highlighted by this admittedly restricted data base. We welcome suggestions for improvements, additions, and especially corrections, for eventual incorporation into an updated version of the review.

A. Applications of *z*-pinch x rays

A most exciting application of flash x rays is microlithography and x-ray microscopy. In these applications the total energy per pulse is less important than the spectral range of photon energies. Lithography, using x rays with $h\nu$ around 1 keV (and a wavelength around 1 nm), can produce sharply defined features of less than 0.1 μm width on electronic materials, due to the small wavelength and to the strongly localized absorption of the photon energy in the photographic resists. Resist exposure takes only 1–3 shots with a small ($\sim$50 kJ electrical) *z*-pinch (Pearlman, 1981/1985a/b; Weinberg, 1986a/b) (or plasma focus; see Kato, 1986). Before *z*-pinch x rays can be used for routine production of microchips (Pearlmann, 1985a/b) it is necessary to resolve difficult problems; these include reducing the size of the x-ray emitting spot, increasing the repetition rate, and protecting the lithographic masks from *z*-pinch debris.

Contact microscopy with soft x rays (Howells, 1985; Kirz, 1985) produces excellent contrast because their photon energies overlap the *K* edges of the low atomic number elements that constitute living matter. A photon energy just above the *K* edge of a given element is attenuated effectively, while a photon with energy just below the *K* edge is relatively unaffected. Hence, the soft x-ray source can be tuned to look at a particular element, obviating the need to enhance contrast by staining with heavy elements that might kill a cell. A 10-ns long flash of x rays from a *z*-pinch has caught a bacterium's activities live (e.g., Bailey, 1982a; Feder, 1984; Weinberg, 1985b). Similar results can be obtained with radiation from laser-produced plasmas.

X-ray spectroscopists use the highly charged ions present in copious quantities in the *z*-pinch for basic atomic physics studies (see, e.g., Striganov, 1983) and, in particular, as a rich source of emission lines (e.g., Burkhalter, 1878, 1979a, 1979b). Highly ionized ions can be made with exploding wires (Dozier, 1977), or vacuum sparks, or by shooting ions through foils; however, the *z*-pinch is unique in its large x-ray output per shot. At present, much ongoing research is devoted to increasing the *z*-pinch x-ray output without softening the x-ray spectrum, or to hardening the spectrum without sacrificing x-ray yield.

B. Qualitative description of *z*-pinch radiation sources

Our *z*-pinch plasmas are usually driven by a capacitor bank with a total stored energy of 1 kJ–10 MJ. The capacitor bank is discharged either directly or through a pulse-shortening network to produce a current peaking at 100 kA–10 MA: the current rise time is typically between 10 ns and 1 μs. Table I contains characteristic parameters for a representative selection of machines used in *z*-pinch work.

A typical *z*-pinch implosion goes roughly as follows. Initially cold material is located a few centimeters away from the diode axis. In the first few nanoseconds of the current pulse the material heats up and ionizes. The resulting pressure expands the plasma, unhindered toward the axis on the inside but constrained by the magnetic field pressure on the outside. Therefore, the plasma accelerates toward the axis. During the implosion the plasma is heated by ohmic and compressional (shock) heating to perhaps $\sim$20 eV. Sometimes the imploding shell is unstable. When the plasma stagnates on axis and the kinetic energy is thermalized the temperature increases steeply, producing a plasma column of $\sim$100 eV or higher. This bulk plasma emits a major fraction of the softer x rays.

After stagnation the pinch disassembles. The plasma can expand unhindered if at disassembly time the current is small. However, if the current is appreciable the stagnated plasma is magnetically confined, with additional ohmic heating, and possibly non-ohmic effects such as accelerated electron beams. In addition, a magnetically confined plasma column is hydrodynamically unstable to sausage and kink modes. The sausage mode results in localized "bright spots," which emit the bulk of the harder x rays. Section II contains a selection of the experimental data on which this description is based (bright spots are shown in Fig. 10).

Section III summarizes the theoretical models sometimes used in prediction and interpretation of experiments. The radiative properties of one-dimensional plasma implosions can be computed with some confidence as long as the plasma remains in various kinds of simplifying equilibrium. Under development but still beyond the state of the art are more complicated effects, notably the nonequilibrium plasma physics of the pinch and the pinch's two-dimensional evolution. Unfortunately, these principal problem areas include x-ray production in the bright spots.

II. EXPERIMENTAL DATA

Experiments with plasma radiation sources (PRS) over the last 10 years have produced an abundance of measurements, much of which remains partly analyzed and unpublished. This section contains a selection of experimental data intended to illustrate particular aspects of the behavior of the *z*-pinch and its radiation output. Abundant data exist in the soft x-ray regime, with photon energy $h\nu$ above $\sim$0.8 keV, because many experiments are motivated by increasing the soft x-ray production, and because these photons are easier to analyze and to measure. Quantitative data in the extreme ultraviolet, here defined as $h\nu$ below $\sim$0.8 keV, are relatively sparse. The parameter space of the data is very large, with four independent output variables (viz., axial and radial position, time, and photon energy); additional variables are the atomic number Z of the *z*-pinch material, load parameters (mass per unit length and initial geometry). In addition, the pinches depend on parameters such as current rise time, peak current, and pulse length related to the pulse power generators, mostly large relativistic electron-beam ma-

chines. Qualitative trends in the data are noted where possible: quantitatively, these trends are not necessarily rigorous, proven theoretically, or accepted by all the workers in the field.

Table I summarizes the parameters of the various machines that supply much of the available data on the PRS. The names of some larger facilities express the speculative nature of the pulse power designs. The machines with the largest power levels are water-filled pulse-shortening lines energized by a high-voltage Marx generator (see Camarcat, 1985). Smaller machines may use a less expensive, lower voltage technology, discharging a single stage of 20–50 kV capacitors into a parallel-plate transmission line insulated with a solid dielectric. The various machines are characterized in Table I by their pulse rise time, the maximum electrical power available to a short-circuit load in the diode, and the peak current. The numerical values are illustrative and will change with machine configuration and diode load even for the same charging voltage; moreover, occasional overhauls and upgrades sometimes increase machine parameters. Reliable operation usually requires usage at less than full power.

Energy delivered to the plasma load is converted into optical (vacuum), ultraviolet, x-ray ultraviolet (XUV), and soft x-ray radiation. At a given power, load geometry, and mass, the higher atomic number elements radiate profusely in the VUV and XUV, with much less output of soft x rays. This radiation, generally below ~ 10 keV, is sometimes accompanied by small amounts of harder x rays.

The XUV radiation pulse is typically much wider than the soft x-ray pulse. For example, the XUV radiation pulse from a krypton gas shell implosion on the Proto II generator at Sandia National Laboratory (Spielman, 1985a), Fig. 2, has a 30-ns-wide precursor followed by a large 30-ns pulse, compared to the ~ 10-ns soft x-ray pulse. As usual, the operational definition of XUV is determined by the detector used, here an x-ray diode with an aluminum cathode and a 2-μm-thick Kimfol filter. This cathode filter combination has a peak response near 270 eV. The soft x-ray signal is measured with a *p-i-n* diode filtered with 25 μm of aluminum; the

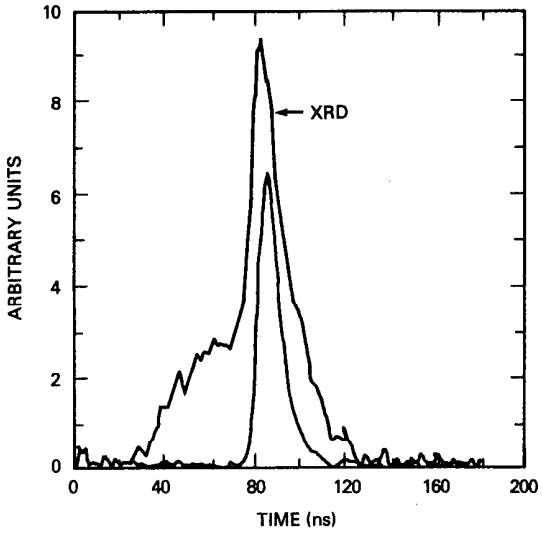

FIG. 2. Pulse shape for XUV radiation measured with a filtered x-ray diode (XRD) and for soft x rays (measured with a filtered *p-i-n* diode) for a krypton implosion on Proto II at SNL (from Spielman, 1985a). The softer the radiation the longer the radiation pulse.

TABLE I. Nominal parameters for some pulse power generators used for imploding *z*-pinches, and a typical value for the radiative energy per pulse in the x-ray lines specified. The data are indicative of but not necessarily equal to the optimum performance: lower values are often used in *z*-pinch research. AFWL: Air Force Weapons Laboratory, Albuquerque, NM. CEA: Commission a l'Energie Atomique, France. IColl: Imperial College of Technology, London, England. KI: Kurchatov Insitute, Moscow, USSR. LANL: Los Alamos National Laboratory, Los Alamos, NM. LLNL: Lawrence Livermore National Laboratory, Livermore, CA. MLI: Maxwell Laboratories, San Diego, CA. NRL: Naval Research Laboratory, Washington, DC. PI: Physics International, San Leandro, CA. SNL: Sandia National Laboratory, Albuquerque, NM. UCI: University of California, Irvine, CA.

Machine name	Location	Nominal power (TW)	Nominal I_{max} (MA)	Nominal x-ray yield (kJ)	Reference
Double Eagle	PI	8	3	15 (Ne *K*)	Dukart, 1983
Blackjack 5	MLI	10	4.6	50 (Ne *K*)	Gersten, 1986
Pithon	PI	5	3		Stallings, 1979
Proto II	SNL	3	9	2.3 (Kr *L*)	Spielman, 1986
Supermite	SNL	2	2	(Ne *K*)	Hsing, 1987
Blackjack 3	MLI	1	1		Riordan, 1981
Gamble II	NRL	1	1.5	4 (Ne *K*)	Stephanakis, 1986
Owl II	PI	1	1		Stallings, 1976
Sidonix	CEA	0.5		>0.5 (Al *K*)	Gazaix, 1984
Shiva	AFWL	1	10	<4 (Al *K*)	Roderick, 1983
ZAPP	LLNL	0.2		(Ar *K*)	Stewart, 1987
	LANL	0.2	0.6		Kania, 1984
	IColl		0.3		Dangor, 1986
Lexis	MLI		0.6	0.02 (Kr *L*)	Pearlman, 1985
	UCI		0.3		Shiloh, 1979
	KI		1.0		Ivanenkov, 1986

peak response of this detector is near 1.5 keV. Other x-ray ranges can be selected by the proper choice of the cathode combined with filter material and thickness (e.g., Young, 1986).

With a sufficiently powerful generator the soft x-ray emission from low atomic number materials is dominated by line radiation from the K shell. For example, Fig. 3 shows three soft x-ray spectra from different axial positions in a neon implosion on Gamble II (Mehlman, 1986). The dominant atomic lines are the Ne IX (He-like) Heα $1s^2$-$1s2p$ at $h\nu = 0.92$ keV and the Ne X (H-like) Hα $1s$-$2p$ resonance line at $h\nu = 1.02$ keV: in the center of the pinch, Fig. 3(b), 42% of the energy is in these lines. Relatively little energy is emitted in the other lines [$\sim 9\%$ for Fig. 3(b)] and in the free-bound continuum with $h\nu \geqslant 1.36$ keV. The energy in all continuum radiation between 0.9 and 1.6 keV is about 50% of the total (2.5 kJ for this shot). The relative strength of the lines can be used to estimate the plasma conditions in the pinch. For this pinch the temperature is ~ 100 eV.

How the spectrum looks qualitatively remains unchanged with a larger generator. Figure 4(a) shows a neon spectrum (Rodenburg, 1985a) measured for an implosion on Double Eagle at ~ 10 times the power of Gamble II. Now the pinch reaches a higher temperature, ~ 300 eV, as evidenced by the spectrum. Now the Heα line is much weaker than the Hα line, which contains over 50% of the soft x-ray energy (total ~ 15 kJ).

In contrast to the neatly separated lines for neon, the implosion of high atomic number elements produces a tangle of overlapping lines. For example, Fig. 4(b) is the spectrum from a nickel wire array on Double Eagle (Rodenburg, 1985b), largely consisting of L-shell lines from Ne-like and higher ionization stages of nickel. About 50% of the energy, in total ~ 44 kJ, occurs in a band between 1.0 and 1.12 keV.

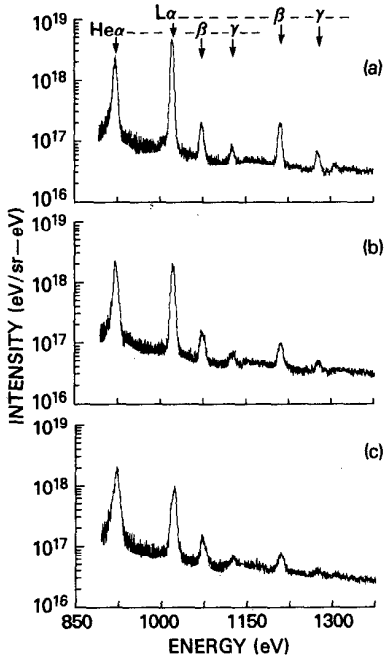

FIG. 3. Experimental soft x-ray spectra at different axial positions in a neon pinch on Gamble II. (a) Near the cathode, (b) midgap between cathode and anode, and (c) near the anode (from Mehlman, 1986).

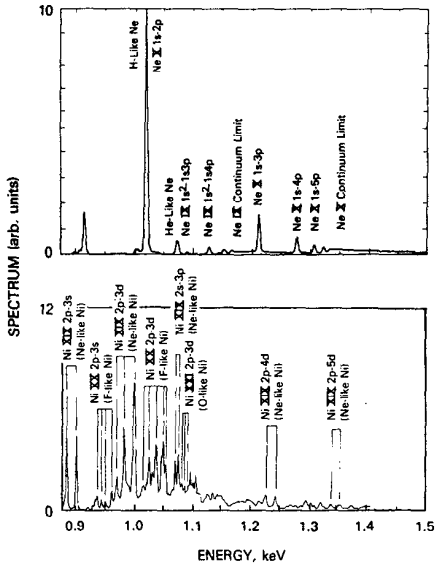

FIG. 4. (a) Experimental soft x-ray spectrum for neon with dominant K-line emission (Double Eagle, from Rodenburg, 1985a). (b) Experimental soft x-ray spectrum for nickel. The individual lines, largely from the L shell, are no longer separated but have merged to a quasicontinuum (courtesy of Dr. R. Rodenburg).

The total energy radiated per shot in soft x rays (in a desired energy band) is an important figure of merit. The maximum value of the yield is often preferred over the typical yield. This practice tends to minimize the shot-to-shot variation, which is typically $\sim 5\%$–10% for the current, but much larger for the radiation output: similar shots can differ in yield by a factor ~ 2. The radiation yield data are typically for optimized experimental parameters and include an unspecified spread. The radiation output is usually determined from the fluence over a small detector, and converted to a total yield under the assumption that the photon fluence is isotropic. However, measurement of the yield versus polar angle θ on a small neon and argon pinch shows that the fluence varies approximately as $1 + \epsilon \cos\theta$, with $\epsilon \sim 0.25$–0.5. Consequently, the fluence perpendicular to the pinch ($\theta = 0$) is twice to four times that along the pinch ($\theta \sim 90°$), although the fluence ratio is not very reproducible from pinch to pinch (Stormberg, 1987).

The yield from various z-pinches is summarized in Fig. 5 (Pearlman, 1985a). The best radiation yield Y_K for K-line photons as function of peak current I is reasonably well approximated by $Y_K \propto I^4$. The scaling of yield with current can be understood easily from the implosion dynamics (Wong, 1982).

The K-line yield decreases rapidly with increasing atomic number Z or with increasing photon energy $h\nu \sim Z^2$. Approximately, the yield varies as $Y_K = \text{const}(I/h\nu)^4$ or $\sim I^4/Z^8$. The strong scaling with Z can be explained from microscopic physics under reasonable assumptions (Apruseze, 1984b).

Other pulsed plasma devices show comparably strong dependencies on the current. For example, the neutron yield from a plasma focus device could vary even more strongly, as I^6, and the neutron yield in a solid deuterium z-pinch even goes as I^{10} (Sethian, 1987). Improvements in pulse power, with corresponding increases in peak current, are bound to

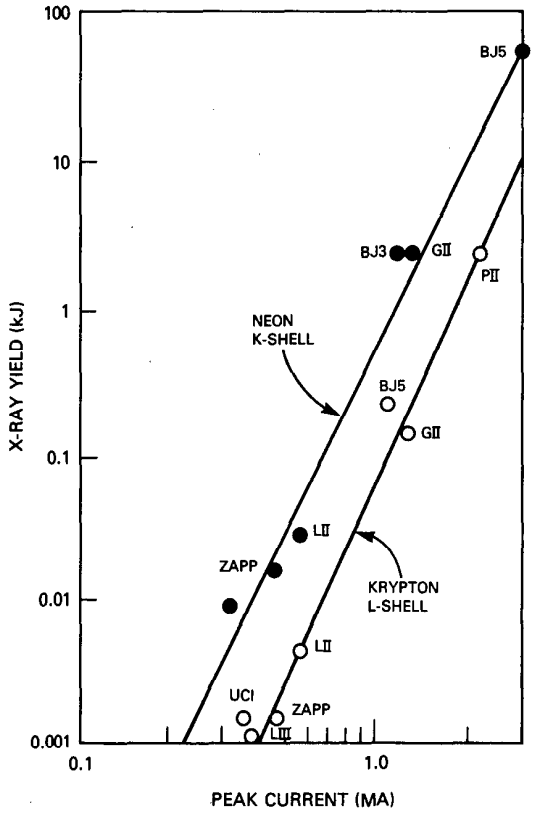

FIG. 5. Optimized radiation yield in neon K lines and krypton L radiation vs peak current I on various pulse power machines (Table I). The yield is proportional to I^4 for both types of radiation (after Pearlman, 1985a).

pay off handsomely in yields from all manner of pulsed power driven plasmas.

Although it is important for x-ray source development to maximize photon output per shot it is equally interesting to pursue alternative goals, e.g., a uniform, linear pinch with controlled plasma conditions for x-ray laser studies (e.g., Dukart, 1983; Wong, 1984; Spielman, 1985b; Stephanakis, 1986). Ease of operation and a moderate price are additional requirements for routine or commercial application (Pearlman, 1985a). Some of the best data on z-pinches has come from innovative diagnostics on smaller machines characterized by high shot rate, ease of modifications, and resources for analysis (e.g., Shiloh, 1978; Marrs, 1983; Kania, 1984; Jones, 1985; Bailey, 1986; Choi, 1986; Stewart, 1987).

A. Z-pinch creation

While PRS diodes differ between machines and applications, the canonical diode for a plasma radiation source consists of a cylindrical rod with a $\sim$1–5 cm radius as the cathode, placed a similar distance from the anode. The cathode sticks out of the pulse line plane such that the UV light from the pinch does not reach the insulators that separate the diode vacuum from the pulseline dielectric. Sketches of actual diode geometries usually accompany the experimental papers (e.g., Stephanakis, 1986; Bailey, 1986; Clark, 1982b/c; Kania, 1984b; Pearlman, 1981; Stallings, 1976). The diode is evacuated to a moderately low pressure, $\sim 10^{-4}$ Torr (0.01 Pa) or less: with appreciably higher diode pressure the gas may break down spontaneously, and becomes more like a plasma focus discharge.

The essential feature of the z-pinch radiation source is the deliberate introduction of the material at the desired location in sufficient quantity to avoid the vacuum spark regime. There is of course a continuous transition between the ultrafast z-pinch and the vacuum spark as the number of electrons per unit length N increases. A value for N may be estimated as follows. In a z-pinch the electrical current I is thought to be collision dominated, while current conduction in a vacuum spark may be dominated by anomalous processes (plasma instabilities leading to high microscopic electric fields, turbulence, etc.). To avoid instabilities the electron thermal velocity v_e should be larger than a typical electron drift speed v_D, with $Nev_D = I$. In the z-pinch regime, therefore, the number of electrons/length $N > I/ev_{\text{th}}$ $\sim I/[ec\sqrt{(T(\text{keV})/500)}]$, which is 6×10^{17} electrons/cm$\times I$(MA) (for $T\sim0.5$ keV).

As the number of electrons per unit length decreases, the vacuum spark gradually transforms into an electron diode. The smallest number of pinch electrons per unit length N_{min} that can carry a current I occurs when all electrons travel with the velocity of light c, i.e., $I = N_{\text{min}}ec$ or $N_{\text{min}}\,(/\text{cm}^3) = 2\times10^{16}\,I(\text{MA})$. If the number of pinch electrons per unit length N is less than N_{min} the pinch electrons must be supplemented by other electrons, presumably emitted from the cathode. For still smaller N, the bulk of the current is carried by these emitted electrons, as in a pure electron diode. In the process, the character of the discharge changes from a resistive diode to a space-charge-dominated diode.

Whether the discharge material is initially a solid, a gas, or a plasma appears to be unimportant for the radiation output of the pinch provided the electrical breakdown is sufficiently uniform. In all cases the material becomes a plasma early into the discharge. However, the initial mass distribution differs for the various phases, and this may be the most important factor in pinch behavior. Connecting the electrodes with thin wires is convenient. However, this restricts the load material to solids such as plastic, Al, Ti, or Fe. A practical problem with wire loads in their replacement after each shot, which usually involves a time-consuming opening of the diode, although this could be avoided by loading the wires in the vacuum under electrostatic guidance (Kania, 1984a).

Six or more wires are theoretically stable (Felber, 1981) against perturbations that destroy cylindrical symmetry. The symmetry in the implosion is apparently important in the production of radiation. With the same load impedance or initial radius and the same mass per unit length, the output from four wires is indeed smaller than with six wires (Stallings, 1976). Experiments to increase the radiation by using 12 or even 24 wires fail to give a substantial improvement. Therefore, six wires are most common, because this minimizes the difficult handling of fragile wires. When the mass/length can be substantial it is unnecessary to use indi-

vidual wires. Instead, thin cylindrical foils can be used (Baker, 1978).

The dominant alternative to wires is the pulsed injection of gas (Shiloh, 1978), often a noble gas but sometimes a molecular compound or a mixture of gases (Bailey, 1982b), and even a fine powder carried in the gas stream. How much material is injected can be varied by changing the pressure behind the pulsed valve, or the time difference between opening the gas valve and firing of the main pulse. Other ways to provide a load include a discharge through a capillary in an insulator (NaF), which injects a solid plasma plume in the diode (Young, 1986). A hollow cylindrical ring of plasma can be shot into the diode using an auxiliary discharge in a metallic foil (Gazaix, 1984). This technique results in mass distributions with well-defined edges in the radial direction. To obtain a uniform mass density in the azimuthal direction, the auxiliary discharge should be sufficiently well behaved.

For a wire load the cathode and anode can be solid conductors, but for a gas puff load one electrode, typically the cathode, contains the gas nozzle and the puff valve. After opening the puff valve the gas pressure slowly builds up to the proper value, but the tenuous leading edge of the gas, streaming at Mach 4–8 (about 0.1 cm/μs) could still be around. To counteract nonuniform gas buildup in the diode the anode should pass this gas into a larger vacuum vessel. Therefore, the anode cannot be a solid plate. Instead, the anode may consist of rods that intercept the gas stream, wires stretched between posts, a conductive mesh, or a honeycomb (e.g., Wessel, 1986).

The amount of gas in the diode is often unknown, although it is sometimes inferred from the implosion time of the pinch material (assuming all material is swept up). Measurements of the gas density after injection, but before the current pulse has arrived, indicate that the initial gas profile is a cone of gas, expanding radially as it moves away from the nozzle (Smith, 1982/1985). The peak density is $\sim 10^{17}$ ions/cm^3 (Smith, 1982/1985; Gazaix, 1984). Once the gas is ionized the electron density is measurable with laser interferometry (Shiloh, 1979).

With wires the initial amount of material is known; however, even with wires the mass per unit length participating in the implosion may differ from the initial value. For example (Benjamin, 1981), an outer layer may blow off the wire and implode during the initial part of the pulse, leaving less mass for the main implosion. The mass cannot be determined unambiguously from the acceleration in the implosion and the measured diode current, because an unknown part of the diode current is contained in the blown-off material. Conversely, electrode material can end up in the z-pinch. When wire and electrode material differ, the additional material is visible through its characteristic radiation, but when electrode and pinch are the same element (e.g., aluminum) the increased mass is hardly noticeable, the only indicator being the difference in behavior of the pinch close to the electrodes as compared with that in the center. Then another electrode material may be tried (Choi, 1986). Also, material from the current return posts may get mixed in with the load gas. Finally, instabilities in the pinch cause flow of material along the axis out of the compressed region, modifying the mass/length still further.

If the material connecting cathode and anode is conductive, metal, or plasma, the current starts to flow as soon as the electrical pulse arrives, and the voltage between the electrodes is largely inductive. However, if the material is nonconductive, sometimes plastic wires but commonly a gas, the voltage between the electrodes builds up rapidly until the material breaks down. Self-breakdown tends to give sparks that evolve into random current channels, possibly affecting the implosion symmetry. Preionization of the gas by external means then improves the implosion. Preionization with UV flashboards is common. Initially the flashboard's UV spectrum peaks at 70 eV, decreasing to 30 eV as the pulse proceeds. The UV is readily absorbed in the gas shell. Also, preionization with rf waves is used. Preionization may be superfluous if the pulse power generator has a sizeable prepulse. Then the ionization from the prepulse appears to have time to spread throughout the gas, as evidenced by a sufficiently symmetric behavior of the implosion.

Additional control over the initial condition of the pinch is obtained by injecting low-energy electrons along the diode axis through a ring in the anode. The effect is seen experimentally in a reduced amplitude of instabilities, and an improved implosion (Ruden, 1987).

After the pulse the diode is filled with an exploding plasma no longer contained by the magnetic field from the current. Anything to be exposed to the x rays must be protected from this blast. Thin foils stop the hot gases but transmit a varying fraction of the x rays. Pressure buildup in the diode can be avoided by careful design of the outer conductor. X-ray diagnostics are typically so far away that fast closing valves can be used in addition to the slits needed in the diagnostics. Additional magnets block the electrons.

It is possible to get a radiating region with special properties by providing special load configurations. X-ray laser studies with z-pinches need a linear, homogeneous plasma region that remains moderately hot during a 0.1–1 ns period. A gas column (Sincerny, 1985) or a foam cylinder (Spielman, 1985b) on axis in addition to the standard load improves the homogeneity of the imploding gas shell. The converse effect is reached by connecting the electrodes with crossed wires, the "x-pinch" (Kolomensky, 1983; Faenov, 1985; Ivanenkov, 1986; their data are summarized by Zakharov, 1987). The intent is to concentrate the available power in a single point, and generate on a small ($\sim$10-GW electrical) generator the plasma conditions usually seen on terawatt machines.

B. A sampling of z-pinch results

This subsection contains a sampling of diagnostic results available in the literature to illustrate particular aspects of the z-pinch. Table II contains many of the available data. Besides these published results there are many more, but qualitatively similar, data available in internal reports outside the limits of this review.

Usually, soft x rays are the intended product of the PRS, and their energy per pulse is commonly measured on each shot. Also available are the overall electrical parameters of

TABLE II. Some data obtained with z-pinches. In the second column the * indicates quantitative data, a *t* theoretical spectra, a *w* data from wires, and an *x* data from the *x*-pinch. Spectra are from the given element (SS is stainless steel). The last column indicates a time or spatially resolved spectrum.

Reference		Pinhole	Soft x-ray spectrum	XUV spectrum	Resolved spectrum
Aranchuk, 1985		W			
Baker, 1978		Al			
Benjamin, 1981		SS			
Bleach, 1982		Ar		Ne,Ar,Kr,Xe	
Bruno, 1983		Al			
Burkhalter, 1978	*		Fe	Fe	
Burkhalter, 1979a	*	Al	Al,Si,Ti	Al,SS	
Burkhalter, 1979b	*	Ar,Kr	Ne,Ar,Kr		
Choi, 1986		Ar			
Clark, 1986	*t*		Ne		
Clark, 1982			Al,Ca,Ti		
Clark, 1983		Ar	Ar	Ar	Ar
Dozier, 1977	*w*	Pt		Cu,Ag,Au	
Dukart, 1983		Kr	Kr	Kr	
Duston, 1981	*t*		Ar	Ar	
Duston, 1984	*t*		Ne,Ar,Kr		
Gersten, 1981	*s*		Ti		
Gersten, 1985		Al(*t*)	Al		
Golts, 1986			Kr		
Hammel, 1985			Ar		
Hares, 1985		Ar		Ar	
Ivanenkov, 1986	*x*	Al,Pd,W		Mo	
Maxon, 1983	*t*			Ar	
Mehlman, 1986	*	Ne	Ne		Ne
Mosher, 1973	*w*	Ti,W	Ti		
Pearlman, 1981			Ar,Kr	Kr	
Riordan, 1981		C,Al,SS,W	Al,SS,Kr	C,Al,SS,Kr,W	
Shiloh, 1977		Ar			
Shiloh, 1978		Ar,Kr			
Spielman, 1984		Kr,Xe	Kr,Xe		
Stallings, 1976		Al	Kr,Xe		
Stallings, 1979		Ar			
Stephanakis, 1986		Ne			Ne
Stewart, 1987			Ar	Ar	Ar
Zakharov, 1983		Al,W	Al		Al

the machine, e.g., the current at the entrance to the diode and the voltage at the vacuum insulator. Spatially resolved x-ray pinhole pictures simply show the spatial location of the emission, without being quantitative in the radiation output. The same is true of streak and framing photography, which provide both time and spatial resolution. Optical or x-ray filters are used with these techniques to give rough spectral discrimination.

Complete and detailed measurements so coveted by theorists are very hard to obtain and seldom published. These measurements include time and spatially resolved XUV and soft x-ray spectra on the same shot, the last column in Table II. Even much simpler diagnostics, e.g., time and spatially averaged but quantitative x-ray spectra such as Figs. 3 and 4, are available on relatively few shots. Table II marks these with a star (*). Most often the spectra are given qualitatively in terms of film density versus photon energy.

From the spectrum much can be inferred about the average plasma properties. Most often the spectrum is measured for the whole length of the pinch, and contains information about the bulk plasma mixed with the bright spots. Slits are used to restrict the axial field of view. However, because the spectra contain time-averaged emission along a line through the pinch, it is still impossible to determine the local plasma state without further data on where and when the plasma emits the radiation of interest. For example, even the single bright spot diagnosed by Hares (1985) is embedded in a blanket of cooler plasma.

The radiation output per pulse increases strongly with generator power and peak current. More power in the generator allows more plasma to be compressed to a higher density and/or a higher temperature, increasing the x-ray output from the bulk of the pinch plasma, but this is not necessarily the reason for the increased yield. Instead, the increased radiation output appears to be primarily related to more and bigger bright spots, or sometimes to a larger density and temperature in each individual bright spot. These statements are anecdotal and will surely need to be modified as more systematic studies are done.

1. Implosion dynamics

Early on in the pulse the *z*-pinch material is ionized and emits visible light. As the pinch progresses and the material gets hotter the photon energy increases until soft x rays are emitted at stagnation. Visible light is conveniently mea-

sured, and thus is an easy way to follow the implosion. Figure 6 is an optical framing photograph of a hollow gas puff z-pinch imploded on the Lexis capacitor bank (Pearlman, 1985a). Although light cannot be emitted without heated z-pinch material there is no definite relation between light and material, and material and current. For example, the whisps or flares visible in the middle frames do not necessarily indicate that the current flows in the whisps. Also, the fact that the edge of the pinch appears sharp and well defined in frames (a)–(c) does not imply that the current path is thin but results from the emission integrated along the chord. However, visible light, material, and current are often related on the assumption that the pinch material is swept up by the magnetic pressure, as in a snowplow.

In the snowplow model frame (a) suggests a slightly flared gas shell with current running on its outside. The irregularities close to the anode at the bottom appear to result from the gas stream hitting the anode rods. As time goes on, axial perturbations in the pinch edge become more prevalent and the pinch shows deviations from axisymmetry [compare frames (b)–(d)]. Subsequently, the perturbations evolve into the flares of frames (d) and (e). The pinch implodes at all axial locations irrespective of the axial structure, stagnating first close to the cathode and only later close to the anode. This phenomenon is called "zippering."

Not much radiation is emitted until the pinch stagnates [frames (e) and (f)]. Optical radiation in frame (e) comes from the cathode, where a sheath of leftover gas or plasma seems to participate in the current conduction. A dark gap separates the cathode from the uniformly radiating central part of the pinch. A pair of flares is still present close to the anode, which is also emitting light. The flares have disappeared in frame (f) but the gap is still present: it pops up again during pinch disassembly, shown in frames (g) and (h). This final stage consists of a beadlike helix as could be expected from an advanced stage of hydrodynamic sausage instability superposed on a kink mode (Bateman, 1978).

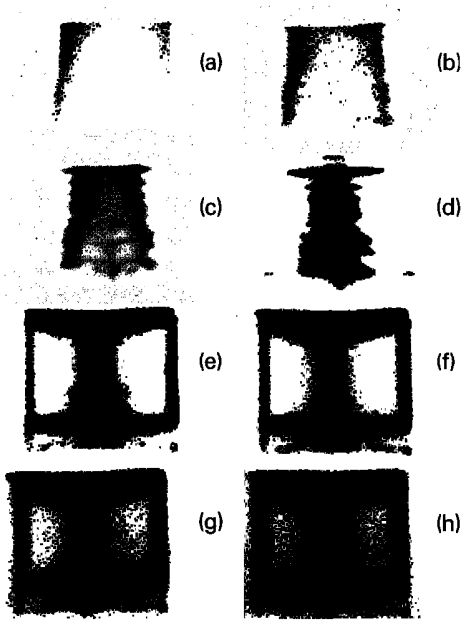

FIG. 6. Implosion sequence of a gas puff z-pinch measured in optical light (from Pearlman, 1985a). The anode-cathode gap is 3 cm, the interframe time is 50 ns.

Is the dynamics of the implosion consistent with all the mass being swept up by the current as if the magnetic pressure were a snowplow (Katzenstein, 1981)? If this were the case, the radial position of the gas sheath as a function of time should be consistent with the acceleration from the $I \times B$ force, and a constant mass per unit length. This can be done by taking an axial slice of the pinch, avoiding axial nonuniformity. For example, Fig. 7 shows the time evolution of a slice perpendicular to the axis in the middle of an argon pinch on a 10-TW pulseline with 100-ns rise time (Clark, 1982c). The "radius of the pinch," both the plasma edge and the current sheath, is then identified with the light emission.

At the beginning of the main current pulse, 50 ns before stagnation, the plasma already has an inward radial velocity obtained from the prepulse. As the pulse progresses the luminosity sheath (arbitrarily defined by the transition between dark and light blue) implodes and thickens at the same time. Stagnation occurs at $t = 0$ ns as defined by the green curve intersecting the axis, but already 10 ns earlier some precursor plasma (light) has reached the axis. For the purpose of comparison with the implosion model the plasma position is defined as the brightest radius in dark blue until 25 ns before implosion, when it changes to the light blue and the green. The comparison is favorable (see Fig. 8): the measured radius $r(t)$ is in good agreement with the acceleration determined from the force $\mu_0 I(t)^2/2\pi r(t)$ and a constant mass per unit length, which is considered as an adjustable parameter. The pinch dynamics has been corroborated in a similar fashion in many other experiments (e.g., Degnan, 1981; Clark, 1982a/b; Bruno, 1983; Bogolubskii, 1986). Use of the mass as an adjustable parameter is almost unavoidable: the mass per unit length of the gas is very hard to measure, and even the mass per unit length of a wire load is uncertain. The value of the current is typically more reliable, even though the current is seldom measured close to the pinch: the magnetic field in a z-pinch can be measured with Faraday rotation (Veretennikov, 1985).

It is important to note that the radiation output cannot be optimized simply by choosing the stagnation time at the peak of the current pulse (Gersten, 1986).

After implosion the pinch at the axial location of the streak radiates strongly for 30 ns in the visible (red in Fig. 7), but the soft x-ray radiation pulse from this particular axial location is much shorter. The soft x-ray pulse from the whole pinch has a full width at half maximum (FWHM) of $\sim$20 ns, compare Fig. 2.

2. Spatial features

Some visible light is generated from the start of the current pulse, while XUV radiation is emitted in a fairly wide pulse around the stagnation time. The spatially averaged soft x-ray pulse is still shorter, Fig. 2, but soft x rays from a given location in the pinch come in an even sharper pulse. For example, Fig. 9 is an x-ray framing photograph of a krypton pinch designed to be linear with minimal zippering (Dukart,

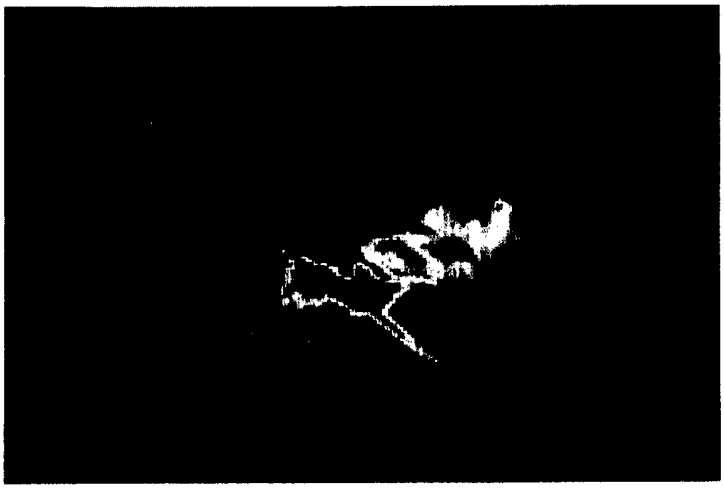

FIG. 7. Optical streak photograph (color plate) showing the radial collapse of argon z-pinch. The picture starts at 170 ns after the beginning of the electrical pulse (see Fig. 8). This initial part of the pulse gives a small initial velocity to the gas; the strongest acceleration occurs just before stagnation. During the contraction the luminosity sheath has a finite width; the final pinch size is about 1 mm. Strong optical emission occurs during about 40 ns (bottom scale) (courtesy of Dr. J. Pearlman: for an uncolored version of this photograph see Clark, 1982c).

1983). A typical axial location strongly radiates soft x rays (blue) during only 2 ns, with the exception of the pinch close to the cathode, where the radiation persists for 10 ns. The total emission from the pinch lasts for about 15 ns. Proper design of the gas nozzle to minimize the zippering can reduce the pulse width from 10 to 4 ns (Hsing, 1987).

Much of the kinetic energy accumulated in the pinch material during run in is converted into optical and XUV photons irrespective of the details of the pinch. In contrast, the soft x radiation is typically emitted by localized bright spots; this radiation is sensitive to the pinch conditions such as current level and atomic number of the load. This point is illustrated in Fig. 10, which compares two sets of pinhole pictures, one in the XUV with photon energy $h\nu$ around a few 100 eV, and the other in soft x rays with $h\nu$ over 1 keV. The left picture is an aluminum pinch ($Z = 13$), and the right is a tungsten pinch ($Z = 74$) (Riordan, 1981). Apart from the atomic number, the pinch conditions were similar, e.g., the same maximum current (~ 1 MA) and an optimum mass per unit length for soft x-ray production ($\sim 150\ \mu g/$

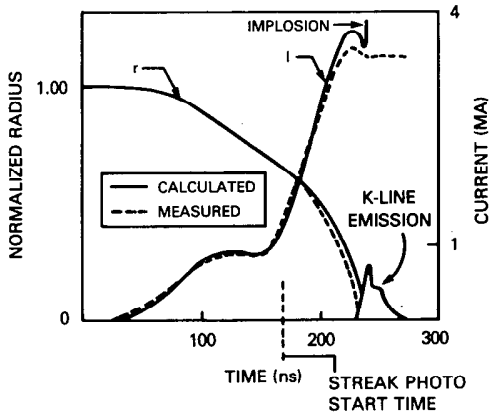

FIG. 8. Measured and calculated load current compared to the measured and calculated radius of the imploding argon pinch in Fig. 7. The K-line x-ray pulse (arbitrary scale) starts 230 ns into the pulse at stagnation (Blackjack 5, after Clark, 1982c).

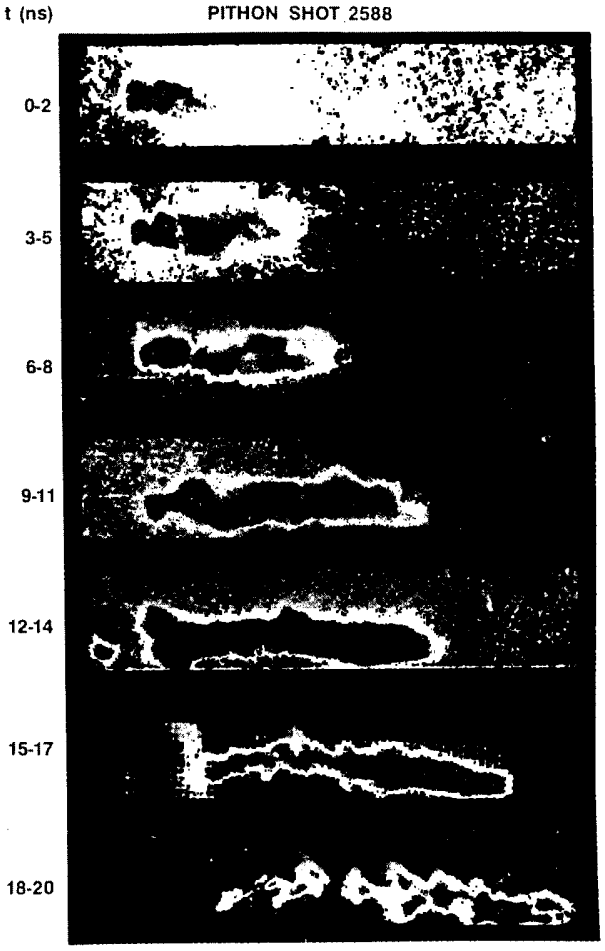

FIG. 9. Time-resolved pinhole photograph in ~ 1.6-keV x rays of a krypton gas puff plasma (Pithon; courtesy Dr. S. L. Wong: for an uncolored version of this photograph see Dukart, 1983).

cm). The XUV emission in both shots comes more or less uniformly from a neighborhood of the axis, but the difference in soft x-ray output is striking, with the hot spots much more pronounced for tungsten. For both materials there is also a weak correlation between the bright spots in the soft x rays and a slight structure in the XUV output.

Similar behavior is seen when the atomic number of the load remains the same but other pinch parameters vary (Riordan, 1981). At the same peak current, increasing the mass per unit length m/l from the optimum for soft x-ray production reduces the number and size of the bright spots, but increases the optical and XUV emission. The pinches still differ even if the implosion time is kept the same by reducing the initial radius r_0 and increasing the mass per unit length to keep mr_0^2/l constant. Figure 11 compares x-ray pinhole pictures under these circumstances for an aluminum pinch (Gersten, 1986). The largest mass per unit length and the smallest initial radius produce a narrow, dense, and strongly radiating pinch, panel (a). Increasing the initial radius by a factor of 2 and decreasing the mass per unit length fourfold gives the wide, tenuous pinch in panel (c). The intermediate case, panel (b), has about half the mass per unit length. The radiation yield decreases from 20 kJ for panel (a) and 4.5 kJ for panel (b), to 0.45 kJ for panel (c). The yields depend somewhat on the pinch temperature, but mostly on the peak density obtained in the pinch. The strong decrease of radiation yield with mass is understandable in part by premature heating of the plasma, which prevents compression to a high density.

The radiation generated by atomic processes in a pinch is sometimes accompanied by detectable amounts of unintended harder radiation, apparently produced by 10–100 keV or even higher energy electrons. These can be generated in the stagnation phase by an (resistive or inductive) electric field along the pinch axis (e.g., Putnam, 1979; Warren, 1987). This bremsstrahlung energy increases with machine power but is never strong enough to dominate the pinch energetics. Moreover, it can be avoided almost completely by increasing the amount of pinch material beyond a critical value. Quantitatively, for a shot with an estimated K-line yield of 20 kJ the bremsstrahlung energy from a thick aluminum anode is estimated at $\leqslant$20 J per pulse (Clark, 1982a). The current in the fast electrons (assumed $\sim$1 MeV) is then something like $\leqslant$60 kA, as compared to a $\sim$3 MA total current through the pinch.

In addition to bremsstrahlung generated at pinch time, a short burst of bremsstrahlung can appear at the start of the current pulse. This phenomenon may be related to the front edge of the magnetically insulated space-charge sheath that carries power to the diode.

A $\sim$20-keV electron beam in the axial direction has been observed directly with differentially filtered Faraday cups (Kania, 1984 b). These fast electrons carry a small fraction ($\sim$20 kA) of the total current ($\sim$600 kA). The atomic radiation excited by these nonthermal electrons could dominate the harder part of the radiation output (Hammel, 1984; Dangor, 1986), but whether this happens in all pinches is an open question at the moment. Spectral diagnostics on a single bright spot shows beam-generated radiation in some cases (Hares, 1985): electron beams accel-

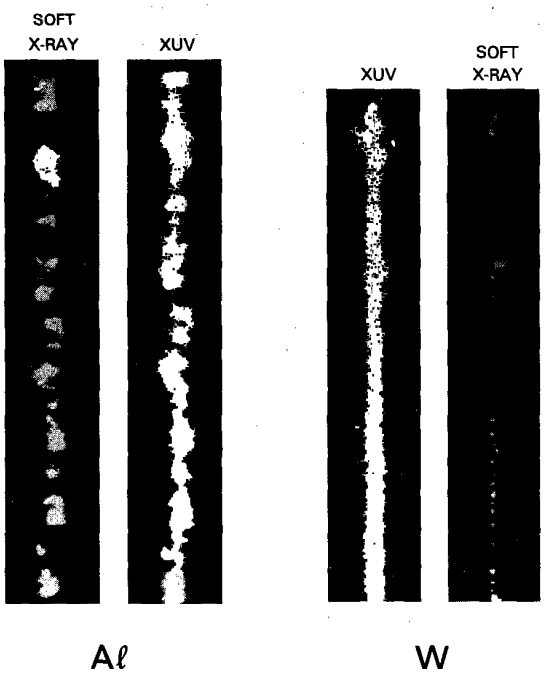

FIG. 10. Time-integrated emission in XUV (inner) and soft x rays (outer) for a 164-μg/cm aluminum pinch and a 141-μg/cm tungsten pinch. The anode-cathode gap is 3 cm, and the nominal current is 1 MA (Blackjack 3, from Riordan, 1981).

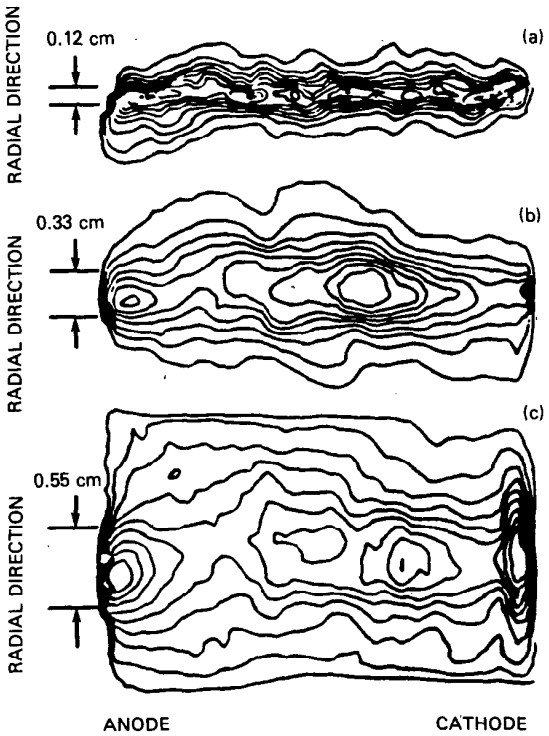

FIG. 11. Contour plots of time-integrated pinhole photographs in soft x rays exceeding 1 keV from aluminum pinches designed to stagnate at the same time during the pulse by changing the intial radius r_0 and the mass per unit length m/l but keeping mr_0^2/l constant. Normalized initial wire array radii r_0 are: (a) 0.5; (b) 0.85; and (c) 1.0 (Blackjack 5, from Gersten, 1986).

erated in the neck of an x-pinch (Zakharov, 1987) produce radiation only in the plasma downstream (between neck and anode). While in z-pinches most of the radiation is excited by thermal electrons, the converse seems to be true in vacuum sparks where most of the radiation output is apparently generated by nonthermal electrons.

Changes in the shape of the current pulse driving the implosion may influence pinch behavior. An example is the use of a plasma erosion opening switch (PEOS) to provide a faster rising current pulse. Figure 12 compares the x-ray emission from a neon gas puff without a PEOS with a similar puff using a PEOS, increasing the current rise time from 2×10^{13} A/s twofold to 4×10^{13} A/s (Stephanakis, 1986; Mehlman, 1986). With the PEOS the bright region is more uniform, even in the individual spectral lines. Moreover, the pinch radius is smaller and there are fewer flares. Other differences in pinch parameters include a smaller mass per unit length for the PEOS case demanded by the shorter time for acceleration, and by the smaller peak current. (1.2 MA vs 0.8 MA).

In shots where stagnation and peak current coincide, the bright spots seem to dominate the soft x-ray emission. In contrast, the bright spots are much less prevalent when stagnation occurs much after peak current. An extreme example is the lack of bright spots in the PEOS shots. There is no systematic study of this phenomenon, but the observation appears consistent with the suspected origin of the bright spots, viz., a sausage instability in the plasma column.

3. XUV radiation

Unlike soft x rays, XUV radiation (e.g., 50–800 eV) shows little structure in space or energy. Emission is typically from a relatively homogeneous column of plasma, without bright spots. The spectrum is rich in lines on top of a continuum. Figure 13(a) compares densitometer traces of a neon XUV spectrum with a krypton XUV spectrum, obtained from the center of the pinch with a grazing incidence spectrometer (many features in these spectra were identified by Bleach, 1983). The continuum consists of merged and broadened lines from different diffraction orders superposed on a background of free-bound continuum radiation. The spectrum becomes smoother with increasing atomic number Z, in part because of the larger number of overlapping lines (Riordan, 1981).

Although the details differ from shot to shot, the XUV emission is qualitatively the same for the different regions of the plasma. Even for different load materials on the same machine the XUV emission is quantitatively similar: for example, the XUV output per shot for krypton ($\sim$30 kJ) is about twice that of neon. Other data on XUV production show comparable features (see Table II).

Quantitative XUV spectra from grazing incidence spectrographs are hard to obtain and therefore rare. Part of the difficulty is the instrument efficiency: in addition, absolute calibration of x-ray film is relatively recent (Henke, 1984a/b; Eidmann, 1986b). However, if only the overall features of

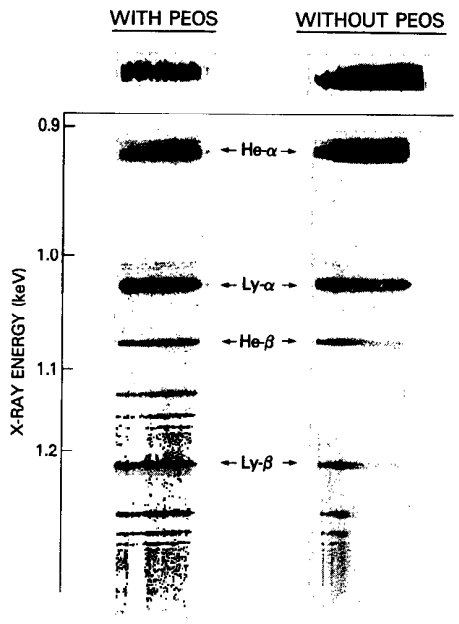

FIG. 12. X-ray pinhole photograph of a neon gas puff implosion without and with the PEOS (Gamble II, from Stephanakis, 1986). The top photograph is spectrally integrated; below these are the spectrally dispersed lines as indicated. Without the PEOS the pinch emits more energetic x rays close to the cathode. The PEOS improves the pinch uniformity.

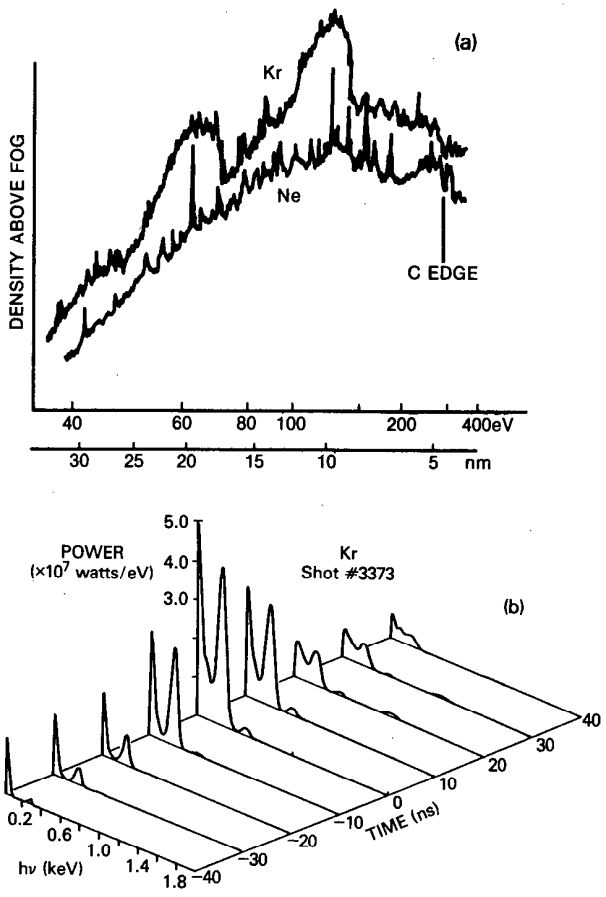

FIG. 13. (a) Densitometer trace of time-integrated XUV spectra at the center of the pinch taken with a grazing incidence spectrometer for neon and krypton (from Bleach, 1983). This reference identifies some of the spectral lines. (b) Time-resolved XUV spectrum from a krypton pinch unfolded from a filtered XRD array (from Bailey, 1986).

the energetics are desired, the spectrum can be determined by the unfolding of differentially filtered x-ray diodes. Figure 13(b) is a time-resolved spectrum of a krypton pinch (output ~0.3 kJ) obtained by this method (Bailey, 1983/6). Note that the radiation is dominated by the XUV below 500 eV, with little radiation above 1 keV.

C. The pinch plasma

With suitable theoretical models, the XUV and soft x-ray spectra can be used to infer average values for the density and temperature of the pinch plasma. These averages are not necessarily an accurate characterization of the plasma when the plasma changes rapidly in time and/or when the plasma is nonuniform, as is usually the case. Axial inhomogeneities, in particular the bright spots, can be diagnosed separately from the bulk plasma with axially resolved spectroscopy (Hares, 1985). The short lifetime of the bright spot can afford some time resolution. However, the spectra are always averaged over the line of sight, and their interpretation yields some radial average. Different spectral features may suggest average plasma parameters that are inconsistent: sometimes inconsistencies can be resolved by assuming that a central core is denser than the surrounding plasma (Gersten, 1986). The following highlights some typical determinations of the plasma parameters.

Laser interferometry followed by Abel inversion (Shiloh, 1979; Bailey, 1982b; Smith, 1985) can be used to measure the electron density as a function of radius during the implosion. For example, Fig. 14 shows that the electron density in the midplane of an argon pinch increases with time as the implosion proceeds, while the shell thickness decreases little. The electron line density N remains constant (at $\sim 6\times 10^{17}$ electrons/cm) until the stagnation point, when N decreases to $\sim 2\times 10^{17}$/cm: the electron density itself peaks at $\sim 10^{19}$ electrons/cm^3. The ion density is not determined by this diagnostic because the ionization fraction is unknown.

The plasma parameters reach their highest value when the material has assembled on axis at and after stagnation. For example, Fig. 15 (Clark, 1983) shows a temporally averaged but axially resolved argon pinch similar to Fig. 6. The radially resolved x-ray emission (lower panel) suggests two bright spots on the anode side of the pinch, and a broader structure on the cathode side. The bright spots, about 2 mm in length and 1 mm radius, appear less pronounced in the radially integrated x-ray emissivity, or in the size of the apparent pinch size in He- and H-like x rays (middle panels). Temperature and density inferred from these data are shown in the top panel: the bright spot is perhaps twice as dense as the adjacent plasma, while the temperature varies relatively little along the pinch. In this case it is reasonable to characterize the plasma by its averaged parameters.

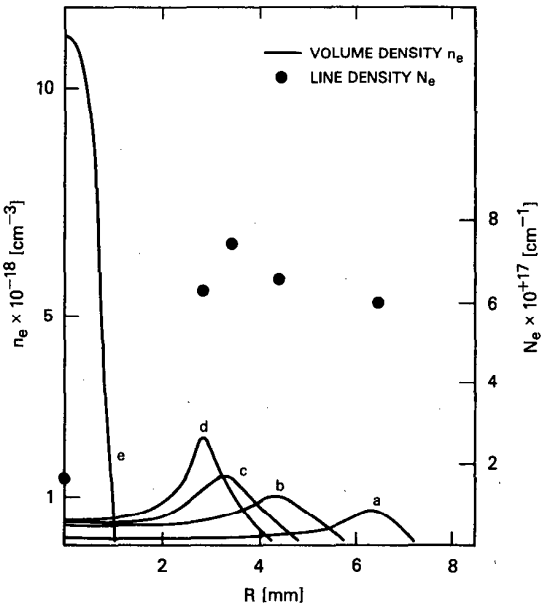

FIG. 14. Time evolution of the radial electron density profile and the electron line density between − 100 ns and stagnation at 0 ns, in 20-ns steps (taken on different shots). The line density remains constant during the pulse. At stagnation the line density decreases, indicating an axial outflow of material consistent with the sausage instability (from Shiloh, 1978a).

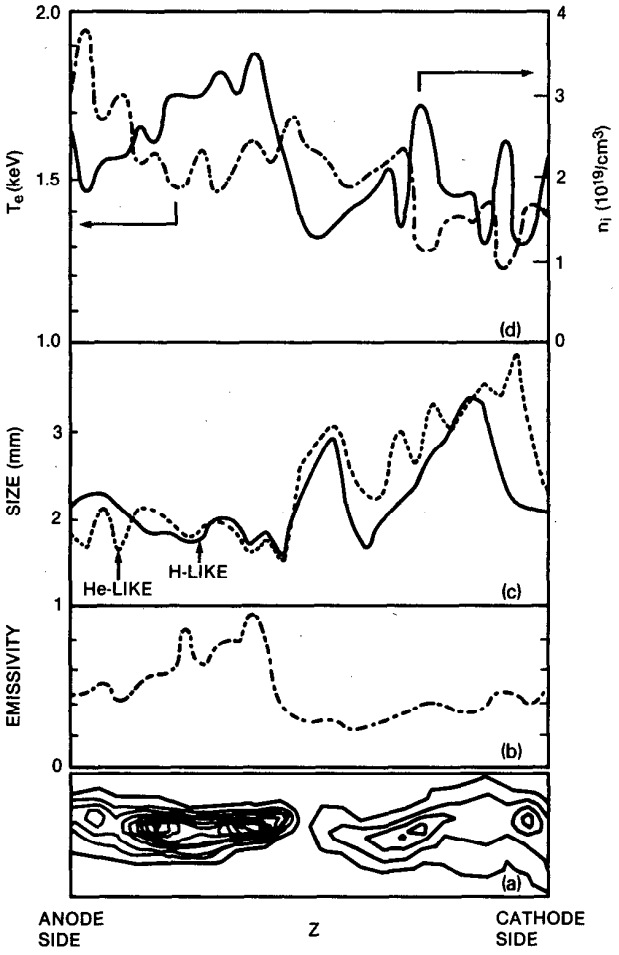

FIG. 15. (a) Contour plot of a pinhole photograph in soft x rays exceeding 1 keV for an argon pinch similar to Fig. 7. (b) Emissivity vs axial distance, (c) time-averaged pinch size for the heliumlike and hydrogenlike argon ions, and (d) axially resolved electron density and temperature from spectral data. The bright spots, at 1/5 and 2/5 of the pinch length close to the anode, show the highest density but unexceptional temperatures (after Clark, 1983, courtesy M. Gersten).

Quite often the bright spots differ substantially from their surroundings, and it is important to diagnose them properly in the light of their dominance in the K-line emissivity. The time-integrated K-line spectrum of a single bright spot in an argon pinch given by Hares (1985) allows a local determination of the bright spot parameters. This bright spot, defined by the strong emission of Ar XVII photons, is ~ 0.1 mm in diameter and 0.6 mm long, much smaller than the bright spot in Fig. 15. There may be a similar amount of material in the two bright spots, because the smaller size is compensated by a much higher electron density, $n_e \sim 3 \times 10^{21}/\text{cm}^3$; electron temperatures are comparable, $T_e \sim 1$ keV. Only 2.5% of the initial line density is in the bright spot: the remainder presumably forms a cooler plasma blanket out to some larger radius, or may have flowed out in the axial direction. A cold core surrounded by a hot plasma is found in exploding wire experiments (Aranchuk, 1986), but here the core radiates little.

The Doppler shift of some XUV spectral lines in a similar argon pinch indeed indicates axial plasma flow, with a flow velocity proportional to the ionic charge state (Stewart, 1987): the peak velocity, 2×10^7 cm/s, is comparable to but smaller than the radial velocity before stagnation [also measurable with Doppler broadening or splitting (Perez, 1980)]. Later in time the pinched plasma develops instabilities and bright spots that emit soft x rays.

Sometimes, but not always, the K lines from heliumlike argon are accompanied by radiation from the K shell of neonlike argon. This unlikely mixture of lines implies the presence of a hot region for the generation of the radiation from the stripped ions, and a cooler region for the generation of inner-shell $K\alpha$'s. In the experiment by Hares (1985) part of the $K\alpha$ radiation from neonlike argon comes from plasma ~ 0.3 mm closer to the anode than the bright spot where the He-like argon is located. Another source of $K\alpha$ lines could be radially outside the bright spot but at the same axial location, or at the bright spot location but at a different time. In addition to the plasma parameters Hares (1985) gives a partial energy balance for this bright spot, including an estimate for the energy in the nonthermal electron component. Similar considerations can be found in Jones (1985).

A systematic and comprehensive determination of the dominant physical processes in the bright spot remains to be performed. Challenging questions include: (i) Is the bright spot in energetic equilibrium? (ii) What is the role of axial mass loss? (iii) How important are runaway electrons? (iv) Why are bright spots comparable in size to the bulk of the pinch for low atomic number Z, but become progressively smaller as Z increases (e.g., Fig. 10)? These and other questions continue to make the radiating z-pinches a fascinating subject.

III. THEORETICAL MODELING

The only theoretical consideration commonly used in pinch experiments is the snowplow model, which predicts the time of implosion from the machine parameters, the load mass, and initial radius. In this model the imploding plasma is assumed to remain an infinitely thin cylindrically symmetric shell. The shell's position $r(t)$ is given by integrating in time the acceleration of a shell element. The magnetic force is the current through this element $dI(t)$ multiplied by the magnetic field $B(r) = \mu_0 I(t)/2\pi r$ divided by the constant mass per unit length dm/l. The current $I(t)$ is determined by a circuit model for the generator coupled to the time-varying inductance of the z-pinch load. One way to avoid the divergence in pinch energy, velocity, and magnetic field at radius $r = 0$ is to cut off the computation when the plasma sheath reaches $\sim 1/10$ of the initial radius (e.g., Katzenstein, 1981). The factor 1/10 is inspired by experimental data and accounts for the expansion of the shell in an approximate way. The snowplow model is successful in determining the implosion time and the kinetic energy at stagnation, but offers little about the radiation output (Gersten, 1986): obviously, better predictive modeling is mandatory.

Roughly speaking, the two theoretical approaches are (i) global estimates of pinch dynamics, stability, and radiation using simplified models as in the early days of plasma physics, and (ii) radiation production and transport computations with detailed ionization dynamic models characteristic of modern astrophysics. The marriage between these two approaches is progressing nicely, but it will be clear from what follows that much remains to be done.

The more sophisticated radiation models are needed to interpret the radiation spectrum in terms of the plasma density, temperature, presence of (nonthermal) electron beams, and other phenomena. This can be done reasonably well with stationary plasma models without hydrodynamic flows. The ultimate goal, to predict the pinch characteristics in detail from first principles, demands time-dependent hydromagnetic models including the radiation energetics.

When the pinch remains cylindrical, the radiation-hydrodynamic models do a very credible job in predicting the total radiation output, including spectral details (Clark, 1986). In contrast, existing models for the "bright spots" are inadequate for an accurate prediction, although some qualitative features can be explained (Vikhrev, 1982).

A typical z-pinch plasma (see Table IV) may be 10 times ionized at 300-eV electron temperature. The energy stored in a 10-times ionized (H-like) ion is ~ 4000 eV, comparable to the thermal energy of the 10 electrons. Moreover, the power into the plasma, compressional and joule heating, is of the same magnitude as the radiative power output. The ionization balance and the radiative power output for z-pinch plasmas are complicated quantities that oftentimes are inadequately approximated by simple models.

Radiation from z-pinches may be heavily influenced by opacity effects, i.e., the multiple absorption and subsequent reemission or destruction of photons before they escape the plasma. Therefore, neither an optically thin (no radiation absorption) nor the blackbody model (equilibrium between the radiation and emitters) applies for the plasma's entire history. Then the proper treatment is to account for all relevant ionization states, the detailed configuration of the plasma, by solving the coupled set of appropriate atomic rate equations including the effects due to photons in conjunction with their transport. There is also the issue of the time scales for the various atomic processes (Kononov, 1977). These tend to be shorter than the hydrodynamic time scale (~ 1–

10 ns), suggesting that the plasma should be in collisional-radiative equilibrium (CRE) for much of its history. Therefore, the CRE approximation is a reasonable choice over much of the plasma's evolution. Details of density and opacity effects on the radiation are shown below.

For typical z-pinch parameters the plasma is highly collisional, with a typical electron-electron collision time $\tau_{ee} \sim 0.1$–1 ps. The collision time is much shorter than the time scale for thermodynamic quantities such as temperature and density, and the bulk of the electron energy distribution is close to a Maxwellian. The plasma transport quantities are moments of the distribution function as given by the standard Braginskiĭ expressions (as corrected by Epperlein, 1986). Likewise, the ionic rates are integrals over cross sections and the Maxwellian electron distribution function that can be determined as functions of temperature.

Deviations from a Maxwellian distribution function are simple to compute, because in the first term expansion of the distribution function a difficult electron-electron collision term can be ignored for a high-Z plasma. This is because the cross section for large-angle Coulomb collisions for electrons with the $\overline{Z} \sim 10\times$ charged ions is Z^2 larger than the electron-electron collision cross section, and the collision frequency $nv\sigma$ is $Z\times$ larger. Hence, most electron collisions are with the almost stationary ions. The distribution function tends to be isotropic and Maxwellian. The transport coefficients for such a Lorentz plasma are available analytically (Epperlein, 1984). However, the radiation from the plasma, connected to the electrons by inelastic collisions, tends to reduce the amount of energetic electrons. For a neon plasma some radiative rates decrease by 50% or more (Pereira, 1988).

The plasma models are not unique to the z-pinch: similar modeling is done wherever strongly radiating plasmas occur. Outstanding examples are laser fusion studies and x-ray laser development. Obviously, each application has its characteristic set of applicable approximations. For example, in laser plasmas the time scales are shorter than in z-pinches, while spatial gradients and plasma densities are usually larger. Features that are specific to those circumstances, e.g., transport coefficients in high-density plasmas (Lee, 1984), or nonlocal heat conduction in large gradients (e.g., Holstein, 1986), may be relevant in limited domains of the z-pinch.

A. Kinematics

Gross properties of the pinch implosion, such as the implosion time or the kinetic energy at stagnation, can be computed reasonably well in a zero-dimensional approximation. The pinch is approximated as either a sheath or a uniform cylinder. Variables may be the plasma radius, and perhaps average plasma parameters such as temperature, density, and pressure. In this section we mention only the kinematic aspects: issues related to the radiation emission appear in Sec. III C.

1. Snowplow model

The radius $r = r(t)$ of a z-pinch of length l with total mass m carrying a current $I = I(t)$ uniformly distributed over a cylindrical shell satisfies

$$\frac{m}{l}\frac{d^2r}{dt^2} = -\frac{\mu_0 I^2}{2\pi(2r)}.$$

The acceleration can be considered as the Lorentz force on a current element $d\theta$, say at azimuthal angle $\theta = 0$, by all other current elements. Only the opposite current element, at $\theta = \pi$ and a distance of $2r$, gives a force through the center. The force from all other elements is not toward the center, but their off-center component vanishes by symmetry; the remaining central force shows an effective distance $2r$ (see also Waisman, 1979).

Typically the current has a maximum I_m, $I = I_m f(\tau)$, where $\tau = t/t_m$, and t_m is a characteristic time. The initial pinch radius is r_m, and $r = r_m R(\tau)$. Then

$$\frac{d^2R}{d\tau^2} = -\left(\frac{\mu_0 I_m^2 t_m^2}{2\pi m/l r_m^2}\right)\frac{f^2}{R},$$

which contains a single parameter (in parentheses) that can be set to unity, thereby defining the characteristic time t_m. Once $f(\tau)$ is given R can be found, seldom analytically but always numerically. The radius $R(t)$ starts at $R = 1$. $R(\tau_0) = 0$ defines the implosion time τ_0, which is finite. Time τ_0 can be bounded from above by keeping $R = 1$ in the magnetic force term. Particularly when the implosion velocity and the current are initially zero this upper bound is a good estimate for the implosion time, because in this case the wires spend most of the implosion time getting up to speed.

During the rise time of the pulse the current is often roughly proportional with time, $f(\tau) = \tau$. Then the implosion radius $R(\tau)$ behaves as in Fig. 16 (solid line, left scale): the dashed lines include the second and third term in the analytical approximation $R = 1 - \tau^4/12 - \tau^8/672 + \ldots$. Clearly, the approximate radius, and therefore the implosion time, are nearly exact. Unfortunately, the energy per unit length $W/l = (mr_m^2/2l)\dot{R}^2$, on the right scale, is not given

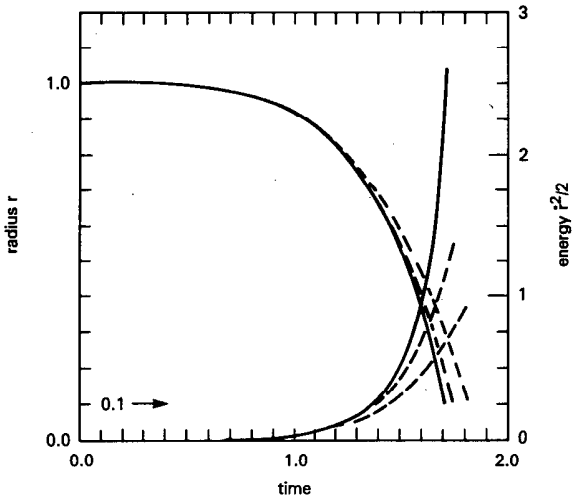

FIG. 16. Pinch radius (left scale) and kinetic energy (right scale) for a snowplow implosion with linear current rise. The solid line is the exact solution, the dashed lines are the two approximations.

accurately by the approximate formulas because much of the pinch energy is acquired toward the end of the implosion. When the current is not given *a priori* but determined with a circuit model it may be advantageous to use circuit parameters in defining the implosion time scale (Katzenstein, 1981). Analytical solutions of the coupled equations are then no longer possible, even though numerical solution is straightforward. However, the moment of inertia per unit length mr_m^2/l always appears in the normalizations, and when this quantity is kept constant the implosions should pick up the energy per unit length, irrespective of the details in the electrical circuit.

The pinch is a time-dependent circuit element with inductance per unit length $L(r,t)/l$. The pinch force per unit length F/l is also the derivative of the inductive energy, $F/l = (\partial L/\partial r)(I^2/2l)$. Integrating over time at constant current leads to an upper bound on the energy transfer, $\Delta L I_m^2/2$, where ΔL is the change in inductance between the initial and final pinch radius. This relation reflects that the power input, $I \times V = I \times dL/dt$, consists of a power with voltage $\partial L/\partial t\, I$, expressing energy transfer to the pinch, and an inductive power with voltage $L\, \partial I/\partial t$ corresponding to the increase of magnetic energy in the diode.

The final pinch radius in the snowplow model is zero but here the model obviously breaks down. Instead, one often assumes that the final pinch radius is 1/10 of the initial radius. The inductance change is then on the order of 4.6 nH/cm, and the energy bound for 1-MA peak current is 2.3 kJ/cm. Besides the kinetic energy in the implosion, the pinch acquires energy from joule heating, a term RI in the circuit. Typically $R \ll \partial L/\partial t$.

Snowplow models are not only useful in defining the approximate mass per unit length needed for a good implosion on a given machine, but also for bringing out the scaling with parameters as stated above. A sobering note is the experimental reality (Gersten, 1986): the radiation output depends less on the kinetic energy of implosion than on the average density at stagnation. A simple formula for the stagnation density in a z-pinch does not exist. A value for the average density can be obtained from the radially resolved density profile computed with a hydrodynamics code, but once such detailed data are available it is silly to revert to the simpler models.

2. Kinematic stability

In practice the individual wires in a multiple wire implosion are never identical or mounted symmetrically, and this asymmetry could spoil the implosion when the perturbation is unstable. Felber (1981) finds that perturbations in radial displacement are stable for six or more identical wires, with growth rate $\omega \leqslant 0$ (or perhaps marginally stable when $\omega = 0$). Perturbations in the axial direction are unstable, but this simply means that the wire parts closer to the center implode faster than those parts of the wire farther away from the center. Introducing an additional current-sharing wire in the center between the wires tends to destabilize the implosion.

The growth rate of perturbations tangential to the (symmetric) reference position is $i\omega$. Consequently, tangential perturbations are marginally stable, or unstable. Fortunately, tangential displacements of the wires do not affect the magnetic force on the wires, and therefore the implosion toward the center is not affected.

Multiple wires are a discrete version of an infinitely thin current sheath; the instability of a current sheath to sausage and kink modes is familiar from hydromagnetic considerations (e.g., Bateman, 1978). The multiple-wire analog of these instabilities becomes important only when the inter-wire forces are large, i.e., when the wires are close together toward the end of the run-in.

While typical wires remain thin compared to the diode size, the wires expand and contract during the pulse (Bloomberg, 1980). Initially, the resistivity is high enough for the current to penetrate, whence the wire expands. Subsequent heating and ionization of the wire material reduces the resistivity and leads to a skin current: the wire contracts. The interaction between the skin current of one wire with the magnetic field from the other wires may describe the blow-off and separate implosion of material observed with heavy wires (Clark, 1982a; Ivanenkov, 1986).

Each wire can pinch by itself while it is accelerating toward the center. Because the instability of a single wire is fast, each individual wire may have pinched before the wires meet on axis, resulting in an inhomogeneous plasma column. Consequently, wire implosions are often less uniform than gas puff implosions.

Blow-off from wires and instability of a single wire both depend on the magnetic field in the wire's immediate neighborhood. In contrast to the magnetic field around an annular conductor, $B_\theta(r) = \mu_0 I(r)/2\pi r$, the field around multiple wires is far from simple, $B_\theta(r,\theta)$ depending strongly on radius and on θ. For symmetric wires the magnetic field is simply a sum over the field from each individual wire if the current is stationary, and the current density in each wire is constant. The opposite case, a rising current in infinitely conducting wires, is found by Waisman (1979). The most interesting case, where the current penetrates the wire during the current rise, remains to be treated.

B. Plasma models

Plasma conditions in z-pinches are often assumed to vary with the radial coordinate in a prescribed way, with one of these a constant. Temperature, density, and radiation output are then, theoretically, functions of time only. This section discusses some of the available models along these lines.

1. Stationary pinch equilibrium

The basic concept is the Bennett pinch, wherein the radial gradient of the (scalar) pressure compensates the Lorentz force $(\nabla p + j \times B)_r = 0$; the Bennett pinch is stationary. Integrating this relation,

$$-\frac{\partial p}{\partial r} = \frac{1}{2\mu_0 r^2}\frac{\partial r^2 B^2}{\partial r},$$

over radius gives an exact relation between the current I, the average electron (ion) temperature $\overline{T}_{e(i)}$, and the number of electrons (ions) per unit length $N_{e(i)}$,

$$\frac{\mu_0 I^2}{4\pi} = 2\pi \int dr\, r[n_i k(T_i + \overline{Z}T_e)]$$

$$\sim N_e k\overline{T}_e \times \frac{\int dr\, rn_e kT_e}{N_e k\overline{T}_e},$$

when ignoring the ion pressure $n_i k\overline{T}_i$. Here $n_{e(i)}$ the electron (ion) density, and the line density is $N_e = 2\pi \int dr\, rn_e$. The average electron temperature is $k\overline{T}_e = \int dr\, rn_e kT_e / \int dr\, rn_e$, and $\overline{Z} = \overline{Z}(\overline{T}_e)$ is the number of electrons per ion. The plasma is quasineutral, $N_e = \overline{Z}N_i$. Numerically, $(N_e/10^{18}\text{cm}^{-1}) \times (\overline{T}_e/\text{keV}) \sim 6 \times (I/\text{MA})^2$. The relation between electron and ion temperature is not always clear, and usually not important. If the electron and ion temperatures are on the same order, the ion pressure is small compared to the electron pressure because typically $\overline{Z} \sim 10$, much larger than unity. Collisions due to ions are unimportant for the ionization equilibrium because the pinch plasma has many more electrons than ions, and moreover the ion velocity vanishes compared to the electron velocity.

An isolated radiating pinch is stationary only on a time scale which is short compared to the cooling down time, i.e., the pinch energy divided by the radiative power. However, the pinch can be rigorously stationary when the energy loss is compensated by energy input from an external source. Power equilibrium was first studied for hydrogen pinches using optically thin bremsstrahlung as the sole radiation loss and joule heating with Spitzer resistivity as the sole energy input. The resulting equilibrium current is known as the Pease–Braginskiĭ current I_{PB}.

For a homogeneous plasma of radius r and average charge state $\overline{Z}$ with a constant current density and total current I, the power gain per unit length is $R/l = I^2\overline{Z} \ln \Lambda / \sigma_0 (T/\text{eV})^{3/2} \pi r^2$; here the Spitzer conductivity is $\sigma_0 (T/\text{eV})^{3/2}/\overline{Z} \ln \Lambda$, with $\sigma_0 = 100\ \Omega^{-1}\,\text{cm}^{-1}$ and $\ln \Lambda \sim 10$ the Coulomb logarithm. The power density in bremsstrahlung (free-free radiation) is $P_{\text{ff}}(\text{W/cm}^3) = X_{\text{ff}} n_e n_i$, where $X_{\text{ff}} = C_{\text{ff}} \overline{Z}^2 (T/\text{eV})^{1/2}$, electron and ion densities in cm^{-3}, and $C = 1.4 \times 10^{-32}\,\text{W cm}^3$ (e.g., Allen, 1973; Book, 1983). The radiative power/length is $\pi r^2 P_{\text{ff}}$.

Balancing these powers in Bennett equilibrium gives

$$I^H_{\text{PB}} \sim 1.4\ \text{MA},$$

independent of atomic number, pinch radius, or temperature (except through the Bennett relation). When the electron density $n_e(r)$ and current density $j(r)$ are no longer constant, a correction factor of order unity comes in:

$$I^2_{\text{PB}} \sim (1.4\ \text{MA})^2 \left[\left(\frac{\int dr\, rj^2}{\int dr\, rn^2} \right)^{1/2} \frac{\int dr\, rn}{\int dr\, rj} \right]$$

(compare Shearer, 1976). In a partly ionized plasma the bremsstrahlung is much weaker than the (free-bound and bound-bound) atomic radiation. The Pease–Braginskiĭ current for a pinch dominated by atomic radiation is therefore much smaller than in a hydrogen pinch, or a hydrogenlike pinch at sufficiently high temperature. In addition, the $T^{1/2}$ temperature dependence of bremsstrahlung no longer combines with the $T^{3/2}$ Spitzer conductivity to give a unique current. For an iron plasma Fig. 17 compares the power coefficients $X = P/n_e n_i$ for bremsstrahlung and total radiation as a function of temperature. At 500 eV the atomic radiation is $100\times$ the bremsstrahlung value; at much higher temperatures $\geqslant 10$ keV bremsstrahlung again becomes appreciable. Radiation emission estimates for many high Z but tenuous plasmas are given by Post (1977) and Jensen (1977).

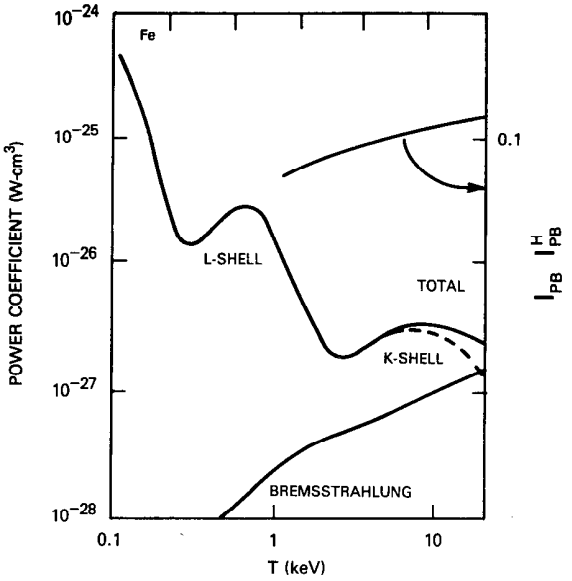

FIG. 17. Bremstrahlung radiation vs temperature (lower line) compared with atomic radiation (free-bound and bound-bound) for iron in the optically thin limit. Atomic radiation dominates in the temperature region of interest (after Jacobs, 1977). The Pease–Braginskiĭ current I_{PB} for an iron pinch is a weak function of the temperature around 0.1 times the Pease–Braginskiĭ current I^{H}_{PB} for hydrogen (right scale).

For comparisons with the Pease–Braginskiĭ current it is convenient to express the total radiation (bound-bound, bound-free, and free-free) by a temperature-dependent function $K(\overline{T})$, which for an optically thin plasma is $K(\overline{T}) = (P_{\text{bb}} + P_{\text{bf}} + P_{\text{ff}})/P_{\text{ff}}$ (Vikhrev, 1977, 1983). Then $I_{\text{PB}} = I^H_{\text{PB}}/[Z(\overline{T})K(\overline{T})]^{1/2}$. As an example, the upper line in Fig. 17 is $I_{\text{PB}}/I^H_{\text{PB}}$ for iron. Obviously, for a radiating pinch the Pease–Braginskiĭ current is much less than 1.4 MA, typically ~ 100 kA.

The Pease–Braginskiĭ current I_{PB} says nothing about the pinch radius because joule heating and optically thin radiation vary with plasma density in the same way. Currents exceeding I_{PB} would not allow power balance and a stationary pinch would not be possible. Instead, the pinch would suffer radiative collapse. The collapse speed depends on the effectiveness of radiative cooling (e.g., Shearer, 1976). In equilibrium the radial profile can be determined from a balance between the heat conductivity, joule heating, and radiative loss [Bobrova, 1987; Scudder, 1983 (for a gas-embedded hydrogen pinch)].

Experimentally the pinches have no problem carrying all the current offered to them by the pulse power, which can exceed $100 \times I_{\text{PB}}$. For dense pinches the current could mainly be carried by a small fraction of the mass outside a cool core, i.e., the mass and current density profile gives a large correction factor (as claimed for an exploding wire, Aranchuk, 1986). For less dense pinches it is more likely that

radiative cooling is too slow for the collapse to occur during the pinch lifetime. A contributing factor may be that radiative cooling is less than expected because the plasma is not in ionization equilibrium (Faenov, 1985). Radiative collapse may be modified by other effects also, e.g., the Bennett pinch condition changes due to electrostatic forces from a net space charge in the pinch (Meierovich, 1982/4).

Without violating the Bennett condition or invoking nonstationary effects, the bright spots (or micropinches) are treated by Vikhrev (1983) using plasma parameters inspired by vacuum sparks. His bright spot model includes the effect of opacity on the radiation, and the contribution of some anomalous resistivity model on the ohmic heating. These modifications introduce a dependence of the Pease–Braginskiĭ current on pinch radius; power equilibrium then defines an equilibrium pinch radius for any current. For an iron pinch at 150 kA the equilibrium radius has a minimum of radius $\sim 1\,\mu$m at an ion line density $N_i \sim 5\times 10^{15}$/cm, corresponding to a Bennett temperature $T = 1$ keV. Micropinches form only in a limited range of line densities: when the initial line density is outside this range the micropinches may form when the line density enters into the contraction regime. Theoretical work emphasizing the final state of the plasma after radiation collapse is discussed extensively by Meierovich (1982/4/6).

Micropinches are frequently quoted in vacuum sparks and z-pinch experiments in the Soviet Union, but perhaps due to different pinch parameters (Gol'ts, 1986] the z-pinch bright spots are not commonly seen in this light in the US. However, it seems likely that bright spots in z-pinches could be described by Vikhrev's radiative contraction model even though the initial line density may be too large: plasma flowing axially out of the neck of an unstable sausage mode reduces the initial line density.

Another basic model is heating under pressure balance, including joule heating but without radiation loss. For a hydrogen pinch with Spitzer resistivity $\eta_H/T^{3/2}$ this condition determines a specific rise in the current versus time $I = I(t)$ (Haines, 1960): for a pinch with atomic number $Z > 1$ the current rise would differ somewhat because the degree of ionization $Z(T)$ and the resistivity constant $\eta_Z = Z(T)\eta_H$ increase with temperature. However, for a radiative pinch such a result is less relevant because radiation losses cannot be ignored.

How close are real z-pinches to these theoretical constructs? The Bennett relation is generally believed to be valid, but the experiments with the best spectroscopic measurements generally do not contain data on the electrical part and vice versa. Table III gathers data from some interesting experiments. The Bennett current I_B as computed from the measured density, radius, and temperature is always smaller than the peak current, but they agree to within a factor ~ 3. The discrepancy is probably due to measurement errors, and to differences between reality and the models. In particular, density and temperature in the pinches vary with radius. Differences remain even when nonuniformity is taken into account by splitting the pinch into a homogeneous core region surrounded by a homogeneous corona, as done by Gersten (1986). Nonc of thc pinches satisfy the Pease–Braginskiĭ condition, except the micropinch (Faenov, 1985) with much higher density than the other pinches. For this pinch the parameters in the experiment appear to agree with theory. The bright spot (Hares, 1985) needs additional heating from an electron beam to explain its parameters. In one model (Jones, 1985) this beam consists of runaway electrons.

2. Simple pinch dynamics

Besides being in stationary equilibrium the z-pinch can support self-similar oscillations. In these somewhat artificial but exact solutions to the equations of ideal MHD, the plasma density, temperature, and magnetic field keep their radial dependence, and all time variation is through the plasma radius. When total current and plasma pressure are not in equilibrium initially the pinch radius oscillates in time (e.g., Felber, 1982), but when bremsstrahlung losses are included the oscillations damp until the pinch degenerates into radiative collapse (Meierovich, 1985). Self-similar dynamics of z-pinches are discussed extensively by Liberman (1986).

TABLE III. Measured data for some well-diagnosed z-pinches. Density and temperature estimates are typically uncertain to a factor ~ 2. Included are the nominal and measured values for one case from Gersten (1986) and the measurements for another. The data from Hares (1985) apply to the bright spot only. Below the line are the same data for a longer pulse micropinch plasma (Faenov, 1985). The Pease–Braginskiĭ current I_{PB} is estimated from the optically thin, low-density plasma emissivity (Jensen, 1977; Post, 1977).

Reference	Atom Z	n_i 10^{18}/cm^3	Temperature (keV)	Diameter (mm)	$\bar{Z}$	N_i 10^{18}/cm	I_{max} (MA)	I_B (MA)	I_{PB}
Mehlman (1986)	10	500	0.15	0.9	8.7	1.0	1.4	0.5	0.06
Gersten (1986) (No. 2)	13	40	0.65/0.3	1.2/3.0	11	0.45/2.4	3.8	1.5	0.07
	(nom)		0.43			17	3.8	4.0	
Gersten (1986) (No. 4)	13	7	1.5/0.75	1.3/3.3	11	0.1/0.5	3.9	1.1	0.08
Hares (1985)	18	3000	beam	0.1	8(?)	1.0	0.25		
Faenov (1985)	13	5000	0.3	0.03	11	0.04	0.15	0.16	0.1

Self-similar oscillations are purely one-dimensional nonequilibrium states representing an axially uniform plasma that contracts and expands in the radial direction only. However, the equilibrium state which supports the oscillations is itself unstable to axial perturbations. In the early days of thermonuclear fusion research with z-pinches these instabilities destroyed plasma confinement, and much effort has gone into determining pinch stability (Bateman, 1978). For radiative pinches, however, the axial plasma flow due to the $m = 0$ sausage mode seems related to the bright spots, and the sausage model's growth rate becomes interesting: nevertheless, most results in this area are for idealized pinches, certainly without radiation effects.

For an idealized pinch with infinite conductivity the current density cannot penetrate the plasma, and remains in an infinitely thin sheath on the outside. For this case the well-known growth rate is $\gamma = C_A/r_0\Gamma$, where $C_A = (B^2/\mu_0\rho)^{1/2}$ is the Alfven speed, r_0 is the pinch radius, and the normalized growth rate $\Gamma = \Gamma(k) \sim O(1)$ is a function of the perturbation wave number $k = r_0\lambda$. In a resistive pinch, however, the current diffuses into the plasma and forms a current sheath with finite thickness (Hussey, 1981). Differences between planar and cylindrical geometry are minor when the current sheath thickness is small compared to the pinch radius (Roderick, 1986). Hwang (1987) treats instabilities in the sheath including the effects of acceleration.

With increasing thickness of the current density sheath the normalized growth rate for the sausage mode decreases (Pereira, 1984), and when the current density is constant throughout the pinch the sausage model is neutrally stable. The kink ($m = 1$) perturbation remains unstable. This instability is of minor interest for radiating pinches, largely because it does not change the mass per unit length in the pinch.

In nonideal MHD the growth rate may be modified by other effects, such as resistive diffusion of the current sheath while the instability is growing, a finite Larmor radius of the ions (Coppins, 1984a, 1984b), and by radiation losses. No definite conclusion is known, although it seems reasonable that radiation losses would increase the sausage growth rate by counteracting an increase in the plasma temperature.

C. Radiation

The theoretical considerations above are valuable for their qualitative insight and guidance into the relevant areas of z-pinch physics. Quantitative prediction of z-pinch behavior, however, is much more demanding, and still in progress. One-dimensional pinch models including hydrodynamics and radiation are in reasonably good shape but of limited use. Remember that the most interesting radiation comes from the bright spot, which is at least two-dimensional. Worse, if electron beams are present the bright spot plasma violates the thermodynamic equilibrium assumptions inherent in the hydrodynamic approximation.

Comprehensive modeling of z-pinch hydrodynamics involves a heavy dose of atomic physics and radiation transport, including related effects such as determination of line profiles. Good introductions are Mihalas (1978) or Cannon (1985). Sobelman (1981) is a relevant research monograph on collisions in plasmas. Recent reviews by DeMichelis (1981, 1984) emphasize radiation from tokamak plasmas but include many references to review articles on specific topics of interest.

The z-pinch plasmas are sufficiently similar to some laser-produced plasmas and x-ray laser media so that many physics issues are the same for both. Much recent literature on the modeling of laser-produced plasma radiation (e.g., Duston, 1980; Apruseze, 1981; Duston, 1983a/b; Duston, 1985b) or x-ray lasers (e.g., Hagelstein, 1983; Apruzese, 1985a; Cochran, 1986; Davis, 1987, 1988) is highly relevant to z-pinches.

1. Fundamentals

In the corona model, describing a low density, optically thin plasma, the ionization fractions f_a are functions of temperature only. This is because each $f_a = n_a/n_i$ (n_a is the density of ions in a specific ionization state a, n_i is the original ion density) is given by a balance between collisional excitation (including ionization) and radiative decay (including radiative recombination), whose rates depend only on temperature. Consequently, the power lost by the plasma in radiation is simply $P = X(T)n_e n_i$ times the plasma volume, where the power coefficient $X(T)$ depends only on temperature. This is no longer true with increasing density, when the decay rate of the excited states must include collisional processes such as collisional recombination. Ultimately, a reasonably complete model for the radiation should be coupled to the implosion hydrodynamics and the instability development in a self-consistent manner. This section discusses the radiation aspects of z-pinches in some detail. Radiative processes are particularly relevant to radiating z-pinches. Typically, the plasma density in a z-pinch (see Table IV) is high enough to modify the ionization fractions from their low density limit. Moreover, the plasma thickness is sufficiently large to make opacity important for the K-shell resonance lines, and certainly for many L-shell lines.

As an example, Fig. 18 shows the power coefficient X_l for line emission from a homogeneous aluminum plasma (Duston, 1981). At $n_i \ll 10^{15}/\text{cm}^3$ the power coefficient peaks around 80 eV (for L-shell radiation); K-shell radiation is maximum around the 1/10 lower second peak around 900 eV. For a typical z-pinch density, $n_i = 10^{19}/\text{cm}^3$, the L-shell peak is comparable to the K-shell peak, which at this density barely changes. At higher densities $\geqslant 10^{21}/\text{cm}^3$ relevant to laser-produced plasmas the power coefficient decreases even more, eventually approaching local thermodynamic equilibrium (LTE). Below ~ 0.8 keV the power coefficient X_l varies approximately as $\sim T^4$, reminiscent of a blackbody. However, for a typical z-pinch plasma at $n_i \sim 10^{19}/\text{cm}^3$ the power coefficient X_l estimated in the LTE approximation is unreliable, $30\times$ too large at 0.2 keV and $10\times$ too low at 1.0 keV. Argon shows a similar decrease in power coefficient with increasing density (Duston, 1982).

For a homogeneous plasma cylinder of 0.05-mm radius and 10^{19} ions/cm^3, see Fig. 19, the added inclusion of opacity gives a threefold reduction in power density $P_l\bar{Z}(T_e)n_i^2$

TABLE IV. Plasma parameters for a canonical pinch, and estimates for the microscopic length and time scales in this plasma. Parameters for other z-pinches may differ an order of magnitude from the values given, and the ordering of length and time scales may reverse.

	Symbol	Equation (MKS)	Typical value
Mass/length	μ		30 μg/cm
Radius	r		1 mm
Current	I		1 MA
Pulse length	τ_p		20 ns
Ions/length[a]	N_i	$\mu \times 2N_A$	10^{18}/cm
Ionic charge	Z		10
Charge/length		$eN_e = Z_e N_i$	1.6 C/cm
Electron temperature	T_e		300 eV
Ion temperature	T_i		300 eV(?)
Electron density	n_e		3×10^{20}/cm^3
Ion density	n_i		3×10^{19}/cm^3
Magnetic field (edge)	B	$\mu_0 I/2\pi r$	200 T
Plasma frequency	ω_{pe}	$(e^2 n_e/\epsilon_0 m)^{1/2}$	10^{15}/s
Gyrofrequency	ω_{ce}	eB/m	3×10^{14}/s
e-e collision time	τ_{ee}		0.5 ps
e-i collision time	τ_{ei}	τ_{ee}/Z	0.05 ps
e-i energy exchange	τ_ϵ	$(M/m)\tau_{ei}$	2 ns
Collisionality		$\omega_{pe}\tau_{ee}$	500
Collisionality (edge)	Ω	$\omega_{ce}\tau_{ei}$	20
Thermal velocity	v_{Te}	$(T_e/m)^{1/2}$	7×10^8 cm/s
Drift velocity	v_D	I/eN_e	10^6 cm/s

[a] Avogadro's number $N_A = 6\times10^{23}$ electrons/g.

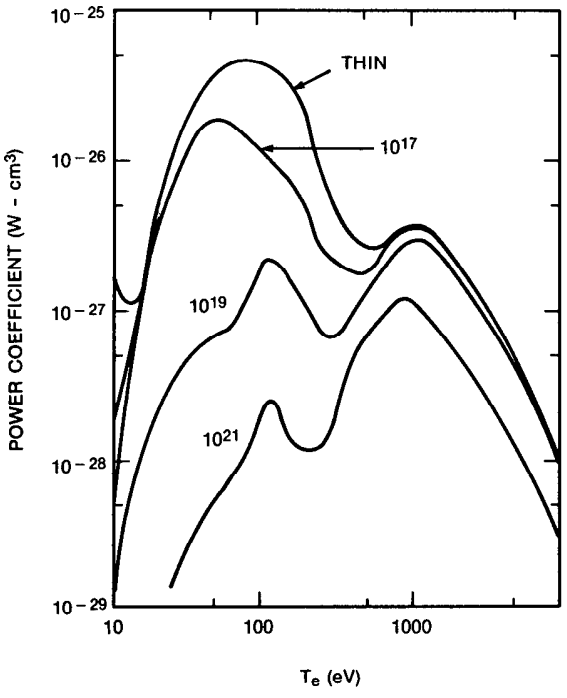

FIG. 18. Line emission power coefficient for aluminum (in the optically thin limit), showing the effect of electron density. Collisional deexcitation reduces the power coefficient around the L-shell peak by an order of magnitude (from Duston, 1981).

at 0.1 keV, but little effect at 1 keV (in contrast to the previous figure this figure includes, besides the lines, the contribution from the continuum). Increasing the cylinder radius to 0.5 mm does not further reduce the power density (the power per unit length would increase 100×). The K-line emission power, at ~1 keV, is unaffected by opacity, al-

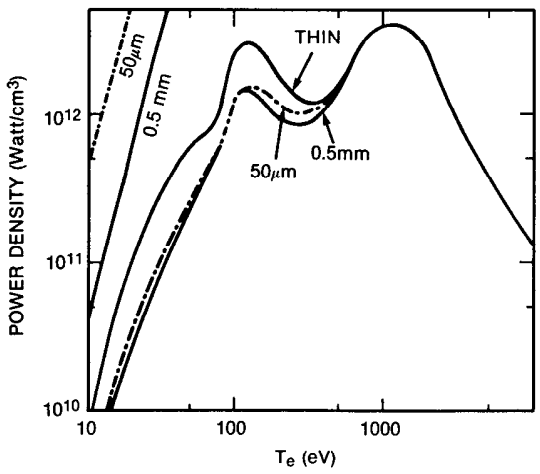

FIG. 19. Radiative power density for a plasma cylinder with 10^{19} aluminum ions/cm^3 in the optically thin limit, and with inclusion of opacity for 50 μm and 0.5 mm radius. Opacity gives a factor 3 reduction in emission at ~200 eV. Blackbody emission would be much stronger, according to the straight lines at left (from Duston, 1981).

though the linewidth increases. The power emitted by this partially transparent plasma is always much less than the equivalent power density for a blackbody, i.e., the power from the blackbody's cylindrical surface divided by the volume $2\sigma_{SB} T_e^4/r$ ($\sigma_{SB} = 10^5$ W/cm^2 eV^4 is the Stefan–Boltzmann constant). Below the L-shell peak a blackbody radiates only one or two orders of magnitude more strongly: at higher temperature the discrepancy is even larger. Opacity effects are invoked to explain the azimuthal dependence of the radiation from a bright spot: the radiation fluence perpendicular to the pinch is perhaps four times larger than the radiation along the pinch, because in the perpendicular direction the photons encounter less plasma (Stormberg, 1987).

Other quantities of interest show corresponding changes from their tenuous and optically thin values, notably the line ratios used as diagnostics of the plasma parameters. Any temperature diagnostic that depends on ionic fractions, such as the Heα to Lyα line ratio, tends to be affected by density effects. For z-pinch parameters a good temperature diagnostic is provided by the dielectronic satellites on the low-energy side of the strong K lines (as in Fig. 3). How this ratio varies for the most prominent satellite line of Lyα for an aluminum plasma is shown in Fig. 20 (Apruzese, 1986); the density has little influence over this line ratio at typical z-pinch densities. How the plasma opacity affects this diagnostic remains to be studied.

Insight into opacity effects can be used to advantage, as demonstrated by Fig. 21, the K-shell power/cm emitted by a uniform plasma cylinder of varying composition but prescribed temperature, radius, and density (Apruzese, 1986). The plasma constituents, neon and sodium, vary such that the total ion density is constant. The neon and sodium K-line photons differ in energy (except for a near-coincidence of the He-line Ne 1-2 with He-like Na 1-4 photons essential to a photopumped x-ray laser). Therefore, the neon K-line opacity decreases as the sodium fraction increases, and each neon photon escapes more easily. Although the number of photons decreases with the number of neon atoms, the decrease is less than proportional due to the opacity effect. On

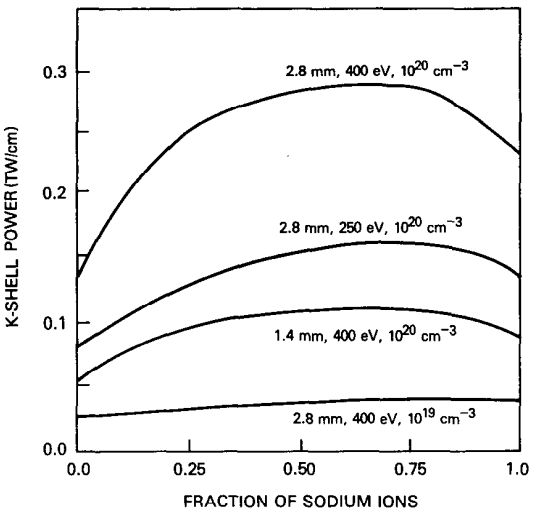

FIG. 21. K-shell radiation power from a sodium-neon plasma vs fractional abundance of sodium for 250- and 400-eV temperature, and for two radii, 1.4 and 2.8 mm. Reduction of opacity increases the radiative power (from Apruseze, 1985b).

balance, the power/cm is maximum for an intermediate plasma composition of around 60% sodium. This result suggests that the radiation output of a z-pinch could be increased by using a mixture of similar elements in order to counter the photon trapping effects from opacity. This assumes that the plasma mixture in an actual pinch reaches the same conditions irrespective of composition.

As an example, a calculation (Duston, 1985a) on mixtures such as He/Kr, with disparate atomic numbers, shows that the high-Z component dominates the radiation yield already when only 10% of the mass is in krypton. The theoretical suggestions are only partly corroborated in experiment (Bailey, 1983/6); a He/Kr pinch with 25% mass in krypton emits less but harder radiation than a pure krypton pinch. Moreover, in the implosion the helium outruns the krypton and stagnates earlier, as explained by Barak (1982).

Fairly rough radiation models can give reasonable results for gross quantities like yields, but the more accurate

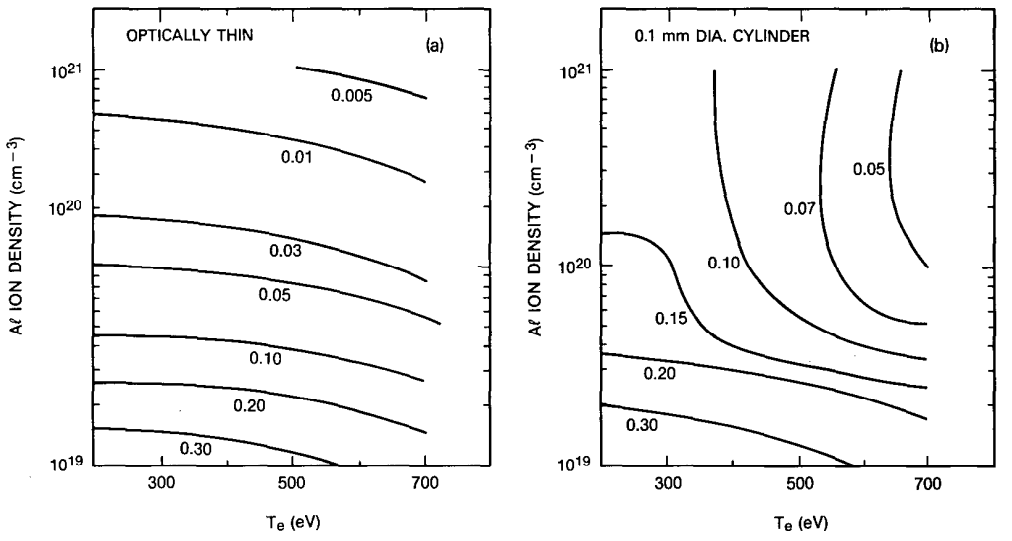

FIG. 20. Contour plots of the intensity ratio between two lines arising from the same ionization state, the $1s^2\ ^1S_0$ to $1s2p\ ^3P_1$ line, and the $1s^2\ ^1S_0$ to $1s2p\ ^1P_1$ line in Al XIII. (a) Optically thin plasma; the line ratio is largely independent of temperature. (b) 0.1-mm-diam cylinder with opacity included; the opacity introduces a strong temperature dependence (from Apruzese, 1986).

models are indispensable when comparing the details of computed spectra with those in experiments. Sometimes the theoretical model must be extended to include radial gradients. A temperature measurement using two line ratios and the continuum temperature produced three somewhat different values when assuming the plasma is a homogeneous cylinder; satisfactory matching of the experimental with a computed spectrum is obtained when the plasma consists of a central hot core surrounded by a colder tenuous corona (Gersten, 1986).

2. One-dimensional radiation hydrodynamics

Many of the important effects mentioned above have been combined into models for the dynamic behavior of z-pinches (Maxon, 1984; Spielman, 1984; Clark, 1986). All are based on the standard hydrodynamic equations; major differences between the models exist in the radiation physics, which is continuously being refined by the various groups.

The one-dimensional computations give satisfactory results when the z-pinch implodes uniformly along the axis. This happens when stagnation is late in the current pulse, and current-driven instabilities have no time to grow into bright spots. An example is a recent computation by Clark (1986). In this work the initial state is a 1-cm-long neon gas shell with uniform density 5×10^{-6} g/cm^3 between an inner radius of 0.55 cm and an outer radius of 1.95 cm. Instead of imploding the shell with magnetic pressure the gas has an initial velocity around 3×10^7 cm/s. This average velocity might be reached late in the current pulse, although in reality the density will be highly nonuniform.

Figure 22 shows the time history of the plasma kinetic energy and the radiative energy for a neon pinch. Plasma ionization and radiation starts already at around 20 ns, when the plasma heats up to $\sim$0.3 keV as the inner edges come together on axis. As the plasma continues to arrive on axis the pinch radiates at an increasing rate, until at about 60 ns into the pulse the kinetic energy has almost completely disappeared into radiation and ionization energy, with the remainder in plasma thermal energy. After stagnation the plasma expands and cools. Slightly more than half the initial energy is radiated away; 30% is left for the kinetic energy of the plasma expansion, and about 10% for thermal and ionization energy.

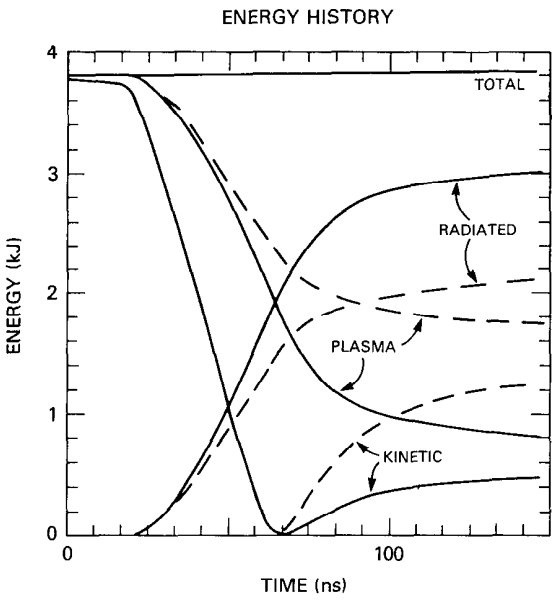

FIG. 22. Temporal development of the kinetic and radiative energy for a 1-cm-long neon shell stagnating on axis according to two different radiation models. The solid lines are from Clark (1986) using a simple model with 27 neon lines, the dashed lines are for a model with over 100 lines (from Clark, 1988). At 70 ns, stagnation, the pinch energy is completely transformed into ionization and thermal energy, or has been radiated. Less than 1/3 of the initial energy is left in pinch disassembly.

The radiation spectrum during stagnation in Fig. 23 is dominated by the neon K-shell lines. The radiation yield in these lines is about 800 J, against $\sim$400 J from the L shell and the continuum each, for a total of 1600 J. It is satisfying that the relative radiation yields in this computation are similar to those obtained in experiments with neon puffs, even though the parameters differ (e.g., Fig. 3; Mehlman, 1986; Stephanakis, 1986).

Quantitative agreement between experiments and computation is claimed by Spielman (1984) between their rare gas implosions and various computational models available to their group. Instead of mocking up the early stage of the implosion by an inwardly coasting plasma, as in Fig. 22, they follow the implosion in time using the experimental current. Possible difficulties with radiative collapse are avoided when including time dependence in the ionization dynamics (Kononov, 1977). Another computation (Maxon, 1984) employed a general-purpose radiation-hydromagnetics code with atomic models that proved insufficiently specific for direct comparison with experiment.

3. Two-dimensional implosion hydromagnetics

Hydrodynamic instabilities during the run-in can destroy the quality of thin foil implosions, but do not affect the implosion of the thicker gas shells. These instabilities and other features of thin foils have been studied mainly in connection with the relevant experiments that are reviewed elsewhere (e.g., Roderick, 1983). A unique feature of these studies is their two-dimensional hydromagnetic computa-

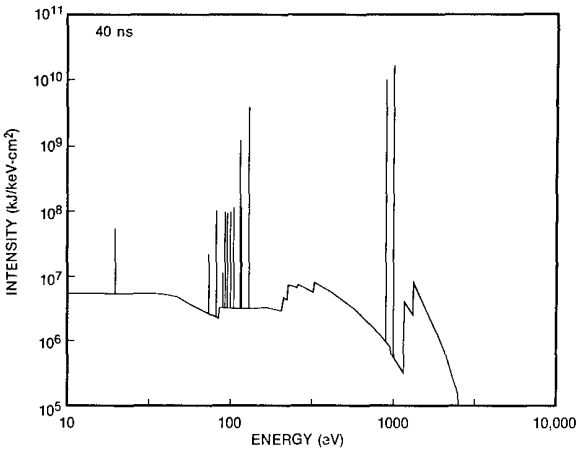

FIG. 23. Neon emission spectrum at 40 ns just before stagnation. Qualitatively the spectrum changes little in time during the implosion, although the power increases with the stagnating volume (from Clark, 1986).

tion of the Raleigh–Taylor instability, its nonlinear saturation, and related problems such as the wall instability (e.g., Hussey, 1980, 1981; Kloc, 1982; Kohn, 1983; Roderick, 1984, 1986b). However, this work omits or underspecifies the radiation physics which is emphasized in this review. Two-dimensional radiation-hydromagnetics models including a satisfactory radiation package are currently being developed, and we look forward to the results.

D. Outlook

This review emphasizes the interplay between the hydrodynamics coupled to the generation and transport of radiation. Certain aspects of radiative z-pinches are well understood in principle, notably various aspects of the radiation modeling of moderately dense and optically thick homogeneous plasmas in collisional-radiative equilibrium; even the time-dependent problem of approach to equilibrium should pose no unsurmountable problem. The hydrodynamics of imploding plasmas can then be considered, including the important effect of energy loss and redistribution due to the radiation. It is no surprise that reasonably complete computations are difficult because of the vast amount of detail that is required.

Basic to these computations are the ionization dynamics and their atomic rates. These depend heavily on the determination of ionic levels and cross sections in a plasma environment, an active area of research in atomic physics: we mention the effect of plasma density on the ionic energy levels, and the computation of the dielectronic recombination cross section.

Next in importance to the cross sections is the electron distribution function $f(v)$: generally $f(v)$ is thought to be Maxwellian, except perhaps along the pinch axis where a small minority of runaway (or beam) electrons may dominate the production of K-line radiation from the bright spots.

Much is known about plasma hydrodynamics without radiation, including the growth rates of axial instabilities in a pinched or imploding plasma, and the self-similar oscillations around the radial equilibrium. The relevancy of these results to radiating z-pinches remains to be evaluated by extending the considerations to include radiation. A similar comment applies to the *hydromagnetics* of radiative z-pinches: how exactly the current penetrates into the plasma is not completely understood.

The major challenge to the theory of radiation z-pinches is to unravel the physics of the bright spot. Apart from any complications with the distribution function the bright spot is certainly two dimensional. Anomalous resistivity due to plasma turbulence (e.g., Papadopoulos, 1977) is often quoted as important in bright spots, but a satisfactory analysis of anomalous processes in the context of a radiative z-pinch does not yet exist. In this we are not alone: theories attempting to model the production of fusion neutrons struggle with similar problems (Vikhrev, 1985, 1986; Trubnikov, 1986).

ACKNOWLEDGMENTS

It is our pleasure to thank our colleagues at NRL and elsewhere for our use of their data. We are particularly grateful to F. C. Young and A. E. Robson for their helpful comments on the manuscript. We acknowledge useful discussions with J. Z. Farber of the Defense Nuclear Agency, and his continuous efforts in support of radiating pinch research. One of us (N.R.P.) would like to thank N. Rostoker for his introduction to pinching. This work was supported by DNA.

Allen, C. W. (1973). *Astrophysical Quantities*, 3rd ed. (Athlone, London).

Alikhanov, S. G., Vasil'ev, V. I., Konov, É. Ya., Koshelev, K. N., Sidel'nikov, Yu. V., and Toporkova, D. A. (1984). "Formation of Micropinches in a High-current Linear Z Pinch with Pulsed Gas Injection," Fiz. Plazmy **10**, 1051 (Sov. J. Plasma Phys. **10**, 605).

Apruzese, J. P. (1981a). "Direct solution of the equation of transfer using frequency- and angle-averaged photon-escape probabilities for spherical and cylindrical gemoetries," J. Quant. Spectrosc. Radiat. Trans. **25**, 419.

Apruzese, J. P., Kepple, P. C., Whitney, K. G., Davis, J., and Duston, D. (1981b). "Collisional-Radiative-Equilibrium Spectroscopic Diagnosis of a Compressed, Optically Thick Neon Plasma," Phys. Rev. A **24**, 1001.

Apruzese, J. P., Davis, J., Duston, D., and Clark, R. W. (1984a). "Influence of Lyman-series Fine-Structure Opacity on the K-shell Spectrum and Level Populations of Low-to-Medium-Z Plasmas," Phys. Rev. A **29**, 246.

Apruzese, J. P. and Davis, J. (1984b). "K-Shell Yield Scaling Law for Conventional PRS Loads," NRL Memorandum Report No. 5406 (unpublished).

Apruzese, J. P. and Davis, J. (1985a). "Kinetics of x-ray lasing by resonant photoexcitation: Fundamentals of pumping power and gain for the Na X-Ne IX system," Phys. Rev. A **31**, 2976.

Apruzese, J. P. and Davis, J. (1985b). "Radiative Properties of Puffed-gas Mixtures: The case of Optically Thick Plasmas Composed of Two Elements with Similar Atomic Numbers," J. Appl. Phys. **57**, 4349.

Apruzese, J. P., Duston, D., and Davis, J. (1986). "K-shell aluminum resonance line ratios for plasma diagnostics using spot spectroscopy," J. Quant. Spectrosc. Radiat. Transfer **36**, 339.

Apruzese, J. P., Mehlman, G., Davis, J., Rogerson, J. E., Scherrer, V. E., Stephanakis, S. J., Ottinger, P. F., and Young, F. C., (1987). "Spectroscopic analysis of sodium-bearing z-pinch plasmas for their x-ray laser pumping efficiency," Phys. Rev. A **35**, 4896.

Aranchuk, L. E., Bogolyubskii, S. L., and Tel'kovskaya, O. V. (1985). "Energy balance of a high-current discharge in an exploding-wire plasma," Zh. Tech. Fiz. **55**, 2222 (Sov. Phys. Tech. Phys. **30**, 1312).

Aranchuk, L. E., Bogolyubskii, G. S., Volkov, G. S., Korolev, V. D., Koba, Yu. V., Liksonov, V. I., Lukin, A. A., Nikandrov, L. B., Tel'kovskaya, O. V., Tulupov, M. V., Chernenko, A. S., Tsarfin, V. Ya. and Yankov, V. V. (1986). "Radiatively cooled z-pinch produced by an exploding copper wire," Fiz. Plazmy **12**, 1324 (Sov. J. Plasma Phys. **12**, 765).

Attwood, D., Halbach, K., and Kim, K.-J. (1985). "Tunable coherent x-rays," Science **228**, 1265.

Bailey, J. Ettinger, Y., Fisher, A., and Feder, R. (1982a). "Evaluation of the gas puff z-pinch as an x-ray lithography and microscopy source," Appl. Phys. Lett. **40**, 33.

Bailey, J., Ettinger, Y., Fisher, A., and Rostoker, N. (1982b). "Gas-puff Z Pinches with D_2 and D_2-Ar Mixtures," Appl. Phys. Lett. **40**, 460.

Bailey, J., Fisher, A., and Rostoker, N. (1986). "Coupling of radiation and hydrodynamics in a z-pinch plasma," J. Appl. Phys. **60**, 1939. Also Ph.D. thesis, "Effect of radiation colling and plasma atomic number on z-pinch dynamics," U. C. Irvine (1983).

Baker, W. L., Clark, M. C., Degnan, J. H., Kiuttu, G. F., McClenahan, C. R., and Reinovsky, R. E. (1978). "Electromagnetic-implosion generation of pulsed high-energy density plasma," J. Appl. Phys. **49**, 4694.

Baksht, R. B., Datsko, I. M., Korostelev, A. F., Loskutov, V. V., Luchinskii, A. V., and Chertov, A. A. (1983). "Nanosecond Electrical Explosion of Thin Wires," Fiz. Plazmy **9**, 1224. (Sov. J. Plasma Phys. **9**, 706).

Baksht, R. B., Datsko, I. M., El'chaninov, A. S., Kovsharov, N. F., Loskutov, V. V., Lushinsky, A. V., Kovalchuk, B. M., Mesyats, G. A., Ratakhin, N. A., Sorokin, S. A., Stasyev, V. P., Sukhov, M. Yu., and Fedusshak, V. F. (1987). "Fast Implosion of Liners" in *Megagauss Technology and Pulse Power Applications*, C. M. Fowler, R. S. Caird, and D. J. Erickson, Ed. (Plenum, New York), p.663.

Barak, G and Rostoker, N. (1982). "Semihydrodynamic model for ion separation in a fast pinch," Appl. Phys. Lett. **41**, 918.

Bateman, G. (1978). *MHD Instabilities* (MIT, Cambridge, MA).
Benford, G. (1978). "Runaway-Electron Model For X-ray Emission in Pinched Discharges," Appl. Phys. Lett. **33**, 983.
Benjamin, R. F., Pearlman, J. S., Chu, E. Y., and Riordan, J. C. (1981). "Measurements of the Dynamics of Imploding Wire Arrays," Appl. Phys. Lett. **39**, 848.
Bleach, R. D. (1980). "X-UV Spectra from Kr XI-XIV," J. Opt. Soc. Am. **70**, 861.
Bleach, R. D., Burkhalter, P. G., Nagel, D. J., and Schneider, R. L. (1983). "Extreme Ultraviolet Emission from Gas Puff Plasmas," J. Appl. Phys. **54**, 1273.
Bloomberg, H. W., Lampe, M., and Colombant, D. G. (1980). "Early Expansion in Exploding Multiple Wire Arrays," J. Appl. Phys. **51**, 5277.
Bobrova, N. A. and Razinkova, T. L. (1987). "Equilibrium states of a z-pinch with emission and thermal conductivity," Fiz. Plasmy **13**, 92 (Sov. J. Plasma Phys. **13**, 53).
Bogolyubskii, S. L., Chernenko, A. S., Dan'ko, S. A., Fanchenko, S. D., Gordeev, E. M., Kalinin, Yu. G., Koba, Yu. V., Korolev, V. D., Kuksov, V. P., Liksonov, V. I., Lukin, A. A., Rudakov, L. I., Shashkov, A. Yu., Shestakov, Yu. I., Smirnova, E. A., Tulupov, M. V., Urutskoev, L. I., and Volkovich, A. G. (1986). "Linear Acceleration Experiments at the 'Module' Facility," in *Proceedings of the Eighth International Conference on High Power Prticle Beams*, Tokyo, Japan.
Book, D. L., Ott, E., and Lampe, M. (1976). "Nonlinear Evolution of the Sausage Instability," Phys. Fluids **19**, 1982.
Braginskiĭ, S. I. (1957). "The behavior of a completely ionized plasma in a strong magnetic field," Zh. Eksp. Teor. Fiz. **33**, 645 (Sov. Phys. JETP **6**, 494).
Brown, G. S. and Lindau, E. E. Eds. (1986). *International Conference on Synchrotron Radiation,* Nucl. Instrum. Methods **246** *passim.*
Bruno, C., Chevallier, J., Delvaux, J., Barbaro, J., Bernard, A., Wolff, G., and David, J. (1983). "X-ray emission efficiency of imploding aluminum wire plasmas," in *Proceedings of Fifth International Conference on High Power Particle Beams,* University of California, San Francisco,CA.
Burhenn, R., Harn., B. S., Gossling, S., Kunze, H. J. and Mielcarski, D. (1984). "Electron temperature scaling in a vacuum spark discharge," J. Phys. D **17**, 1665.
Burkhalter, P. G., Dozier, C. M., Stallings, C., and Cowan, R. D. (1978). "X-ray Line Emission and Plasma conditions in Exploded Fe Wires," J. Appl. Phys. **49**, 1092.
Burkhalter, P., Davis, J., Rauch, J., Clark, W., Dahlbacka, G., and Schneider, R. (1979a). "X-ray line spectra from Exploded-Wire Arrays," J. Appl. Phys. **50**, 705.
Burkhalter, P. G., Shiloh, J., Fisher, A., and Cowan, R. D., (1979b). "X-ray spectra from a gas-puff z-pinch device," J. Appl. Phys. **50**, 4532.
Bykovskii, Yu. A. and Lagoda, V. B. (1982). "Local High-temperature Plasma Formations in a High-current Pinching Discharge," Zh. Eksp. Teor. Phys. **83**, 114 (Sov. Phys. JETP **56**, 61).
Camarcat, N., Delvaux, J., Etlicher, B., Mosher, D., Raboisson, G., and Perronnet, A. (1985). "Electrical pulsed power generators of the 1 TW class," Laser and Particle Beams **3**, 415.
Campbell, E. M., Hunt, J. T., Bliss, E. S., Speck, D. R., and Drake, R. P. (1986). "Nova experimental facility," Rev. Sci. Instrum. **57**, 2101.
Cannon, C. J. (1985). *The Transfer of Spectral Line Radiation* (Cambridge University Press, Cambridge, MA).
Chapin, D. L, Duderstadt, J. J., and Bach, D. R. (1974). "Numerical Studies of Exploding-Wire Plasmas," J. Appl. phys. **45**, 1726.
Choi, P., Dangor, A. E., Deeney, C., and Challis, C. D. (1986). "Temporal development of hard and soft x-ray emission from a gas-puff z pinch," Rev. Sci. Instrum. **57**, 2162.
Cilliers, W. A., Datla, R. U., and Griem, H. R. (1975). "Spectroscopic measurements on vacuum-spark plasmas," Phys. Rev. A **12**, 1408.
Clark, R. W., Davis, J., and Cochran, F. L. (1986). "Dynamics of imploding neon gas-puff plasmas," Phys. Fluids **29**, 1971.
Clark, R. W. and Davis, J. (1988). (unpublished).
Clark, W., Wilkinson, M., Rauch, J., and LePage, J. (1982a). "X-ray Measurements of Imploding Wire Plasmas," J. Appl. Phys. **53**, 1426.
Clark, W., Gersten, M., Katzenstein, J., Rauch, J., Richardson, R., and Wilkinson, M. (1982b). "Aluminum, Calcium, and Titanium Imploding Plasma Experiments on the BLACKJACK 5 Pulse Generator," J. Appl. Phys. **53**, 4099.
Clark, W., Richardson, R., Brannon, J., Wilkinson, M., and Katzenstein, J. (1982c). "The Dynamics of Imploding Argon Plasmas," J. Appl. Phys. **53**, 5552.
Clark, W., Gersten, M., Tanimoto, D., Kolb, A., Pearlman, J., Rauch, J., Richardson, R., Riordan, J., and Wilkinson, M. (1983). "Imploding Plasma Pinches Driven by High Power Generators," in *Proceedings of Fifth International Conference on High Power Particle Beams 1983,* University of California, San Francisco, CA, 1983.
Colloque, (1986). J. Phys. (Paris) Colloq. **C6 S-47** *passim.*
Coppins, M., Bond, D. J., and Haines, M. G., (1984a). "On the Vlasov fluid stability of the $m = 0$ mode in a pure z pinch," J. Plasma Phys. **32**, 1.
Coppins, M., Bond, D. J., and Haines, M. G. (1984b). "A Study of the Stability of the Z Pinch Under Fusion Conditions Using the Hall Fluid Model," Phys. Fluids **27**, 2886.
Dangor, A. E. (1986). "High density z-pinches," Plasma Physics and Controlled Fusion **28**, 1931.
Davanloo, F., Bowen, T. S., and Collins, C. B. (1987). "Scaling to high average powers of a flash x-ray source producing nanosecond pulses," Rev. Sci. Instrum. **58**, 2103.
Davis, J. and Blaha, M. (1982). "Level Shifts and Inelastic Electron Scattering in Dense Plasmas," J. Quant. Spectrosc. Radiat. Transfer **27**, 307.
Davis, J. and Whitney, K. G. (1976). "Line Emission in Al XI as an Optical Diagnostic in Laser-Heated Plasmas," J. Appl. Phys. **47**, 1426.
Davis, J., Apruzese, J. P., Agritellis, C., and Kepple, P. (1987). "Argon puff gas soft X-ray laser," in *Radiative properties of hot, dense matter III,* edited by B. Rozsnyai, C. Hooper, R. Cauble, R. Lee, and J. Davis (World Scientific, Singapore).
Davis, J., editor (1988). IEEE Plasma Sci., *Special issue on x-ray lasers* (to be published).
DeMichelis, C. and Mattioli, M. (1981). "Soft-x-ray spectroscopic diagnostics of laboratory plasmas," Nucl. Fusion **21**, 677.
DeMichelis, C. and Mattioli, M. (1984). "Spectroscopy and impurity behavior in fusion plasmas," Rep. Prog. Phys. **47**, 1233.
Degnan, J. H., Reinovsky, R. E., Honea, D. L., and Bengtson, R. D. (1981). "Electromagnetic Implosions of Cylindrical Gas 'Shells,' " J. Appl. Phys. **52**, 6550.
Dorokhin, L. A., Smirnov, V. P., Tulupov, M. V., and Tsarfin, V. Ya. (1984). "Laser Studies of Exploding Wires," Zh. Tekh. Fiz. **54**, 511. (Sov. Phys. Tech. Phys. **29**, 304).
Dothan, F., Riege, H., Boggasch, E., and Frank, K. (1987). "Dynamics of a z pinch for focusing high-energy charged particles," J. Appl. Phys. **62**, 3585.
Doucet, H. J., Etlicher, J. P., Furtlehner, and Gazaix, M. (1983). "The 'Needle Plasma,' A soft X-Rays-Initiated, Gas Embedded Z-Pinch Computational and Experimental Approaches," in *Proceedings of the Fifth International Conference on High Power Particle Beams,* University of California, San Francisco, CA.
Dozier, C. M., Burkhalter, P. G., Nagel, D. J., Stephanakis, S. J., and Mosher, D. (1977). "High Ionization States in Exploded-Wire Plasmas," J. Phys. B **10**, L73.
Dukart, R., Wong., S. L., Dietrich, D., Fortner, R., and Stewart, R. (1983). "Studies of an imploding plasma x-ray laser," in *Proceedings of Fifth International Conference on High Power Particle Beams,* University of California, San Francisco, CA.
Duston, D. and Davis, J. (1980). "Self-Absorption of Heliumlike Satellite Lines in High-density Fusion Plasmas," Phys. Rev. A **21**, 932.
Duston, D. and Davis, J. (1981). "Soft-X-ray and X-ray Ultraviolet Radiation from High-Density Aluminum Plasmas," Phys. Rev. A **23**, 2602.
Duston, D. and Davis, J. (1982). "Density Effects on the Spatial Emission of a High Temperature Argon Plasma," J. Quant. Spectrosc. Radiat. Transfer **27**, 267.
Duston, D., Clark, R. W., Davis, J., and Apruzese, J. P. (1983a). "Radiation Energetics of a Laser-Produced Plasma," Phys. Rev. A **27**, 1441.
Duston, D., Rogerson, J.E., Davis, J., and Blaha, M. (1983b). "Dense Plasma Effects on *K*-shell Dielectronic Satellite Lines," Phys. Rev. A **28**, 2968.
Duston, D., Davis, J., and Agritellis, C. (1985a). "Radiative Properties of Puffed-Gas Mixtures," J. Appl. Phys. **57**, 785.
Duston, D., Clark, R. W., and Davis, J. (1985b). "Effects of radiation on spectra, gradients, and preheat in laser-produced plasmas," Phys. Rev. A **31**, 3220.
Eidmann, K. and Kishimoto, T. (1986a). "Absolutely measured x-ray spectra from laser plasmas with targets of different elements," Appl. Phys. Lett. **49**, 377.
Eidmann, K., Kishimoto, T., Herrmann, P., Mizui, J., Pakula, R., Sigel, R., and Witkowski, S. (1986b). "Absolute soft x-ray measurements with a transmission grating spectrometer," Laser and Particle Beams **4**, 521.
Epperlein, E. M. (1984). "The accuracy of Braginskiĭ's transport coefficient for a Lorentz plasma," J. Phys. D **17**, 1823.

Epperlein, E. M. and Haines, M. (1986). "Plasma transport coefficients in a magnetic field by direct numerical solution of the Fokker-Planck equation," Phys. Fluids **29**, 1029.
Faenov, A. Ya., Khakhalin, S. Ya., Kolomensky, A. A., Pikuz, S. A., Samokhin, A. I., and Skobelev, I. Yu. (1985). "Superdense high-temperature exploded-wire plasma observations in a high-current vacuum diode," J. Phys. D **18**, 1347.
Feder, R., Pearlman, J. S., Riordan, J. C., and Costa, J. L. (1984). "Flash x-ray microscopy with a gas jet plasma source," J. Microsc. **135**, 347.
Felber, F. S. and Rostoker, N., (1981). "Kink and Displacement Instabilities in Imploding Wire Arrays," Phys. Fluids **24**, 1049.
Felber, F. S. (1982). "Self-similar oscillations of a *z*-pinch," Phys. Fluids **25**, 643.
Felber, F. S., Liberman, M. A., and Velikovich, A. L. (1985). "Methods for Producing Ultrahigh Magnetic Fields," Appl. Phys. Lett. **46**, 1042.
Finken, K. H. (1983). "Untersuchungen an Dichten *Z*-Pinch-Plasmen (Investigations of dense *z*-pinch plasmas)," Fortschr. Phys. **31**, 1.
Gazaix, M., Doucet, H. J., Etlicher, B., Furtlehner, J. P., Lamain, H., and Rouillé, C. (1984). "A New Method to Produce an Annular Cylindrical Plasma for Impoding Plasma Experiments," J. Appl. Phys. **56**, 3209.
Gerritsen, H. C., van Brug, H., Bijkerk, F., and van der Wiel, M. J. (1986). "Laser-generated plasma as soft x-ray source," J. Appl. Phys. **59**, 2337.
Gersten, M., Rauch, J. E., Clark, W., Richardson, R. D., and Wilkinson, G. M. (1981). "Plasma Temperature Measurements from Highly Ionized Titanium Imploding Wire Plasmas," Appl. Phys. Lett **39**, 148.
Gersten, M., Clark, W., Rauch, J. E., Wilkinson, G. M., Katzenstein, J., Richardson, R. D., Davis, J., Duston, D., Apruzese, J. P., and Clark, R. (1986). "Scaling of Plasma Temperature, Density, Size, and X-Ray emission above 1 keV with Array Diameter and Mass for Aluminum Imploding-Wire Plasmas," Phys. Rev. A **33**, 477.
Gerusov, A. V. and Imshennik, V. S. (1985). "Radiative cooling of a *z*-pinch discharge in a deuterium-neon mixture during the collapse of the cylindrical plasma," Fiz. Plazmy **11**, 568 (Sov. J. Plasma Phys. **11**, 332).
Glibert, K. M., Anthes, J. P., Gusinow, M. A., Palmer, M. A., Whitlock, R. R., and Nagel, D. J. (1980). "X-ray Yields of Plasmas Heated by 8-ns Neodymium Laser Pulses," J. Appl. Phys. **51**, 1449.
Gol'ts, E. Ya, Koloshnikov, G. V., Koshelev, K. N., Kramida, A. E., Sidel'nikov, Yu. V., Vikhrev, V. V., Ivanov, V. V., Palkin, A. A., and Prut, V. V. (1986). "A high-temperature micropinch in a discharge with a current of 1 MA," Phys. Lett. A **115**, 114.
Hagelstein, P. L. (1981). Ph.D. thesis, "Physics of short wavelength laser design," UCRL-53100 (unpublished). Also, "Review of Radiation Pumped Soft X-ray Lasers," Plasma Phys. **25**, 1345 (1983).
Haines, M. G. (1960). "The Joule heating of a stable pinched plasma," Proc. R. Soc. London **76**, 250.
Haines, M. G. (1982). "The Physics of the Dense *Z*-Pinch in Theory and in Experiment with Application to Fusion Reactor," Phys. Scr. **T2/2**, 380.
Haines, M. G. (1983). "Ion Beam Formation in an $m = 0$ Unstable Z Pinch," Nucl. Instrum. Methods **207**, 179.
Hammel, B. A. and Jones, L. A. (1984). "Effects of the Internally Produced Nonthermal Electrons on the Temperature Diagnostics of a Hollow Gas Shell Z Pinch," Appl. Phys. Lett. **44**, 667.
Hares, J. D., Marrs, R. E., and Fortner, R. J. (1985). "An Absolute Measure of Heating by Suprathermal Electrons in a Gas Puff *Z*-Pinch," J. Phys. D **18**, 627.
Henke, B. L., Kwok, S. L., Uejio, J. Y., Yamada, H. T., and Young, G. C. (1984a). "Low-energy x-ray response of photographic films. I. Mathematical models," J. Opt. Soc. Am. B **1**, 818.
Henke, B. L., Fujiwara, F. G., Tester, M. A., Dittmore, C. H., and Palmer, M. A. (1984b). "Low-energy x-ray response of photographic films. II. Experimental characterization," J. Opt. Soc. Am. B **1**, 828.
Holstein, P. A., Delettrez, J., Skrupsky, S., and Matte, J. P. (1986). "Modeling nonlocal heat flow in laser-produced plasmas," J. Appl. Phys. **60**, 2296.
Howells, M., Kirz, J., Sayre, D., and Schmahl, G. (1985). "Soft x-ray microscopes," Phys. Today (August 22).
Hsing, W. W. and Porter, J. L. (1987). "Measurements of axial nonuniformities in gas-puff implosions," Appl. Phys. Lett. **50**, 1572.
Hussey, T. W., Roderick, N. F., and Kloc, D. A. (1980). "Scaling of magnetohydrodynamic instabilities in imploding plasma liners," J. Appl. Phys. **51**, 1452.
Hussey, T. W. and Roderick, N. F. (1981). "Diffusion of Magnetic Field into an Expanding Plasma Shell," Phys. Fluids **24**, 1384.
Hussey, T. W., Matzen, M. K., and Roderick, N. F. (1986). "Large-Scale-Length Nonuniformities in Gas Puff Implosions," J. Appl. Phys. **59**, 2677.
Hwang, C. S. and Roderick, N. F. (1987). "Potential flow model for the hydromagnetic Raleigh–Taylor instability in cylindrical plasmas," J. Appl. Phys. **62**, 95.
Ivanenkov, G. V. (1984). "Electron Runaway and Plasma Pinching in a High-current Diode," Dokl. Akad. Nauk SSSR **282**, 1106. (Sov. J. Plasma Phys. **10**, 680.
Ivanenkov, G. V., Kolomensky, A. A., Pikuz, S. A., Samokhin, A. I., and Zakharov, S. M. (1986). "*Z*-Pinch in a High-Current Diode," in *Proceedings of the Eighth International Conference on High Power Particle Beams*, Tokyo, Japan.
Jacobs, V. L., Davis, J., Kepple, P. C., and Blaha, M. (1977). "The influence of autoionization accompanied by excitation on dielectronic recombination and ionization equilibrium," Ap. J. **211**, 605.
Jensen, R. V., Post, D. E., Grasberger, W. H., Tarter, C. B., Lokke, W. A. (1977). "Calculations of impurity radiation and its effects on tokamak experiments," Nucl. Fus. **17**, 1187.
Jones, L. A., Finken, K. H., Dangor, A., Källne, E., and Singer, S. (1981). "A Laser Initiated, Gas-Embedded Z Pinch: Experiment and Computation," Appl. Phys. Lett. **38**, 522.
Jones, L. A. and Kania, D. R. (1985). "Temporally and spatially resolved x-ray emission from a collapsing gas shell *z*-pinch plasma," Phys. Rev. Lett. **55**, 1993.
Kania, D. R. (1984a). "Device for Loading Thin Wires in a Vacuum," Rev. Sci. instrum. **55**, 39.
Kania, D. R. and Jones L. A. (1984b). "Observation of an Electron Beam in an Annular Gas-Puff *Z*-Pinch Plasma Device," Phys. Rev. Lett. **53**, 166.
Kato, Y. and Be, S. H. (1986). "Generation of Soft X rays Using a Rare Gas-Hydrogen Plasma Focus and its Application to X-ray Lithography," Appl. Phys. Lett. **48**, 686.
Katzenstein, J. (1981). "Optimum Coupling of Imploding Loads to Pulse Generators," J. Appl. Phys. **52**, 676.
Kirz, J. and Rarback, H. (1985). "Soft x-ray microscopes," Rev. Sci. Instrum. **56**, 1.
Kloc, D. A., Roderick, N. F., and Hussey, T. W. (1982). "A simple model for plasma temperature in imploded hollow plasma liners," J. Appl. Phys. **53**, 6706.
Koch, E. E. Ed. (1983). *International Conference on Synchrotron Radiation*, Nucl. Instrum. Methods **208** *passim.*
Kodama, R., Okada, K., Ikeda, N., Mineo, M., Tanaka, K. A., Mochizuki, T., and Yamanaka, C. (1986). "Soft x-ray emission from ω_0, $2\omega_0$, and $4\omega_0$ laser-produced plasmas," J. Appl. Phys. **59**, 3050.
Kohn, B. J., Roderick, N. F., and Beason, C. W. (1983). "Two-dimensional Numerical Simulation of an Inductively Driven Imploding Foil Plasma," J. Appl. Phys. **54**, 4348.
Kolomensky, A. A., Lebedev, A. N., Papadichev, V. A., Pikuz, S. A., and Yablokov, B. N. (1983). "Generation and acceleration of multicharge and negative ions in high-current diodes and by means of collective effects," *Proceedings of the International Conference on High Power Particle Beams*, University of California, San Francisco, CA, pp. 533–539.
Kononov, É. Ya., Koshelev, K. N., and Sidel'nikov, Yu. V. (1977). "Spectra of multiply ionized iron atoms in a low-inductance vacuum discharge: time-varying ionization model for the 'plasma-point,'" Fiz. Plazmy **3**, 663 (Sov. J. Plasma Phys. **3**, 375).
Kononov, É. Ya., Koshelev, K. N., and Sidel'nikov, Yu. V. (1985). "X-ray Spectroscopic Study of Micropinches in a Low-Inductance Vacuum Spark," Fiz. Plazmy **11**, 927 (Sov. J. Plasma Phys. **11**, 538).
Korop, E. D., Meĭerovich, B. É., Sidel'nikov, Yu. V., and Sukhorukov, S. T. (1979). "Micropinch in a High-Current Diode," Usp. Fiz. Nauk. **129**, 87 (Sov. Phys. Usp. **22**, 727).
Kühne, M. and Wende, B. (1985). "Vacuum UV and Soft X-ray Radiometry," J. Phys. E **18**, 637.
Lee, T. N. and Elton, R. C. (1971). "X Radiation from Optical and Inner-Shell Transitions in a Highly Ionized Dense Plasma," Phys. Rev. A **3**, 865.
Lee, T. N. (1974). "Solar-Flare and Laboratory Plasma Phenomena," Astrophys. J. **190**, 467.
Lee, T. N. (1975). "High-density Ionization with an Intense Linear Focus Discharge," Ann. NY Acad. Sci. **251**, 112 .
Lee, Y. T. and More, R. M. (1984). "An electron conductivity model for dense plasmas," Phys. Fluids **27**, 1273.
Liberman, M. A. and Velikovich, A. L. (1986). "Self-similar motions in *z*-

pinch dynamics," Nucl. Fusion **26**, 709.
Marrs, R. E., Dietrich, D. D., Fortner, R. J., Levine, M. A., Price, D. F., Stewart, R. E., and Young, B. K. F. (1983). "Time and Space Resolved Vacuum-ultraviolet Spectroscopy of an Argon Gas-Puff Z Pinch," Appl. Phys. Lett. **42**, 946.
Maxon, S. and Wainwright, T. (1984). "Radiation spectra from an imploding argon gas puff," Phys. Fluids **27**, 2535.
Mehlman, G., Burkhalter, P. G., Stephanakis, S. J., Young, F. C., and Nagel, D. J. (1986). "Quantitative x-ray spectroscopy of neon z-pinch plasmas," J. Appl. Phys. **60**, 3427.
Meĭerovich, B. É. (1982). "Electromagnetic Collapse. Equilibrium of a Dense Pinch," Phys. Rep. **92**, 83.
Meĭerovich, B. É. (1984). "Electromagnetic Collapse. Problems of Stability, Emission of Radiation and Evolution of a Dense Pinch," Phys. Rep. **104**, 259.
Meĭerovich, B. É. (1985). "Self-similar model of the radiative compression of a z-pinch," Fiz. Plazmy **11**, 1446 (Sov. Phys. Plasma Phys. **11**, 831).
Meĭerovich, B. É. (1986). "Toward the realization of electromagnetic collapse," Usp. Fiz. Nauk. **149**, 221 (Sov. Phys. Usp. **29**, 506).
Michette, A. G., Cheng., P. C., Eason, R., Feder, W., O'Neill, R. F., Owadano, Y., Rosser, R. J., Rumsby, P., and Shaw, M. J. (1986). "Soft x-ray contact microscopy using laser plasma sources," J. Phys. D **19**, 363.
Mihalas, D. (1978). *Stellar Atmospheres*, 2nd ed. (Freeman, San Francisco, CA).
Mochizuki, T., Yabe, T., Okada, K., Hamada, M., Ikeda, N., Kiyokawa, S., and Yamanaka, C. (1986). "Atomic-Number Dependence of Soft-X-Ray Emission from Various Targets Irradiated by a 0.53-μm-wavelength Laser," Phys. Rev. A **33**, 525.
More, R. M. (1982). "Electronic Energy-Levels in Dense Plasmas," J. Quant. Spectrosc. Radiat. Transfer **27**, 345.
Mosher, D., Stephanakis, S. J., Vitkovitsky, I. M., Dozier, C. M., Levine, L. S., and Nagel, D. J. (1973). "X-Radiation From High-Energy-Density Exploded-Wire Discharges," Appl. Phys. Lett. **23**, 429.
Mosher, D., Stephanakis, S. J., Hain, K., Dozier, C. M., and Young, F. C. (1975). "Electrical Characteristics of High Energy-Density Exploded Wire Plasmas," Ann. NY Acad. Sci. **251**, 632.
Nagel, D. J., Brown, C. M., Peckerar, M. C., Ginter, M. L., Robinson, J. A., McIlrath, T. J., and Carroll, P. K. (1984). "Repetitively pulsed-plasma soft x-ray source," Appl. Opt. **23**, 1428.
Nagel, D. J. (1982). "Potential characteristic and applications of x-ray lasers," in *Advances in x-ray spectroscopy: Contributions in honour of Professor Y. Cauchois*, edited by C. Bonnelle and C. Mande (Pergamon, New York).
Negus, C. R. and Peacock, N. J. (1979). "Local regions of high-pressure plasma in a vacuum spark," J. Phys. D **12**, 91.
Nicolosi, P., Jannitti, E., and Tondello, G. (1981). "Soft X-ray Emission of Continua from Laser Produced Plasmas," Appl. Phys. B **26**, 117.
Papadopoulos, K. (1977). "A review of anomalous resistivity for the ionosphere," Rev. Geophys. Space Phys. **15**, 113.
Pearlman, J. S. and Riordan, J. C. (1981). "X-ray Lithography Using a Pulsed Plasma Source," J. Vac. Sci. Technol. **19**, 1190.
Pearlman, J. S. and Riordan, J. C. (1985a). "Bright discharge plasma sources for x-ray lithography," Proc. SPIE **537**, 102.
Pearlman, J. S., Riordan, J. C., and Kolb, A. C. (1985b). "A bright pulsed x-ray source for soft x-ray research and processing applications," Radiat. Phys. Chem. **25**, 709.
Pease, R. S. (1957). "Equilibrium characteristics of a pinched gas discharge cooled by bremsstrahlung radiation," Proc. Phys. Soc. London B **70**, 11.
Pépin, H., Fabbro, R., Faral, B., Amiranoff, F., Virmont, J., Cottet, F., and Romain, J. P. (1985). "The X-Ray Emission, Ablation Pressure, and Preheating for Foils Irradiated at 0.26 μm Wavelength," Phys. Fluids **28**, 3393.
Pereira, N. R., Rostoker, N., and Pearlman, J. S. (1984). "Z-Pinch Instability with Distributed Current," J. Appl. Phys. **55**, 704.
Pereira, N. R. and Whitney, K. G. (1988). "Non-Maxwellian electron energy distribution due to radiation in a z-pinch," to be published in Phys. Rev. A.
Perez, J. D., Chase, L. F., McDonald, R. E., Tannenwald, L., and Watson, B. A. (1981). "Subkilovolt x-ray radiation from an argon plasma," J. Appl. Phys. **52**, 670.
Phillion, D. W. and Hailey, C. J. (1986). "Brightness and duration of x-ray line sources irradiated with intense 0.53-μm laser light at 60 and 120 ps pulse width," Phys. Rev. A **34**, 4886.
Post, R. S., Johnson, D. J., and Stephanakis, S. J. (1978). "Nonthermal infrared radiation from exploding wire plasmas," Plasma Phys. **20**, 1039.
Post, D. E., Jensen, R. V., Tarter, C. B., Grasberger, W. H., and Lokke, W. A. (1977). "Steady-state radiative cooling rates for low-density, high-temperature plasma," At. Data Nucl. Data Table **20**, 397.
Potter, D. (1978). "The Formation of High-Density Z-Pinches," Nucl. Fus. **18**, 813.
Putnam, S., Stallings, C., Childers, K., Schneider, R., Rothe, I., Creedon, J., Bailey, V., and Young, T. S. T. (1979). "Recent Developments in Fast Z-Pinch Plasma Production Using Superterawatt Generators," in *Proceedings of International Conference on High-Power Particle Beams*, Santa Fe, NM, 1979.
Riordan, J. C., Pearlman, J. S., Gersten, M., and Rauch, J. E. (1981). *Sub-Kilovolt X-ray Emission from Imploding Wire Plasmas*, AIP Conference proceedings, edited by D. Attwood and B. Henke (APS, New York), Vol. 75.
Robson, A. E. (1987). "A Bibliography of the linear z-pinch," Naval Research Laboratory document, Washington, DC (unpublished).
Rodenburg, R., Wong, S., Koppel, L., and Burr, L. (1985a). "Neon Source Optimization on Double-Eagle," in *Proceedings of the 1985 International Conference on Plasma Science.*
Rodenburg, R., Wong, S., Koppel, L., and Burr, L. (1985b). "Observation of L-Series X-Ray Spectra Radiated by a High Temperature Nickel Plasma," presented at The 27th Annual Meeting, Plasma Physics Division, American Physical Society (unpublished).
Roderick, N. F., Kohn, B. J., McCullough, W. F., Beason, C. W., Lupo, J. A., Letterio, J. D., Kloc, D. A., and Hussey, T. W. (1983). "Theoretical Modeling of Electromagnetically Imploded Plasma Liners," Laser and Particle Beams **1**, 181.
Roderick, N. F. and Hussey, T. W. (1984). "A model for the saturation of the Raleigh-Taylor instability," J. Appl. Phys. **56**, 1387.
Roderick, N. F. and Hussey, T. W. (1986a). "Magnetic diffusion smoothing with application to the hydromagnetic Raleigh-Taylor instability," J. Appl. Phys. **59**, 662.
Roderick, N. F. (1986b). "Diffusion of azimuthal magnetic fields into a cylindrical plasma," J. Appl. Phys. **60**, 1269.
Rozsnyai, B. F. (1982). "An Overview of the Problems Connected with Theoretical Calculations for Hot Plasmas," J. Quant. Spectrosc. Radiat. Transfer **27**, 211.
Ruden, E., Rahman, H. U., Fisher, A., and Rostoker, N. (1987). "Stability enhancement of a low initial density hollow gas-puff z-pinch by e-beam preionization," J. Appl. Phys. **61**, 1311.
Scudder, D. W. (1983). "Steady-state radial heat conduction in a z-pinch," Phys. Fluids **26**, 1330.
Seeley, J. F. and Lee, T. N. (1984). "Density Measurement in a Vacuum-Spark-Discharge Microplasma from the Inner-Shell Excitation of Satellite Transitions," Phys. Rev. A **29**, 411.
Sethian, J. D., Robson, A. E., Gerber, K. A., and DeSilva, A. W. (1987). "Enhanced stability and neutron production in a dense z-pinch plasma formed from a frozen deuterium fiber," Phys. Rev. Lett. **59**, 892. [erratum Phys. Lett. **59**, 1790].
Shearer, J. W. (1976). "Contraction of Z pinches Actuated by Radiation Losses," Phys. Fluids **19**, 1426.
Shiloh, J., Fisher, A., and Rostoker, N. (1978). "Z Pinch of a Gas Jet," Phys. Rev. Lett. **40**, 515.
Shiloh, J., Fisher, A., and Bar-Avraham, E. (1979). "Interferometry of a Gas-Puff Z-Pinch Plasma," Appl. Phys. Lett **35**, 390. Also, Ph.D. thesis, "High density z-pinch," UC Irvine, 1978.
Sincerny, P., Wong, S., Buck, V., Gilman, C., and Sheridan, T. (1985). "Pulsed Compression with an Imploding Gas Puff," in *Proceedings of IEEE 5th Pulsed Power Conference* (unpublished).
Skowronek, M. and Romeas, P. (1985). "Experimental Study of the Current Penetration in a Dense Z Pinch," J. Appl. Phys. **57**, 2519.
Smith, R. S., Doggett, W. O., Roth, I., and Stallings, C. (1982). "Supersonic Gas Shell for Puff Pinch Experiments," Appl. Phys. Lett. **41**, 572.
Smith, R. S. and Doggett, W. O. (1985). "Experimental characterization of a puff-gas z-pinch plasma prior to implosion," Appl. Phys. Lett. **46**, 1128. Also, Ph.D. thesis, North Carolina State University, Raleigh, 1985.
Solov'ev, L. S. (1984). "Dynamics of a Cylindrical Z pinch," Fiz. Plazmy **10**, 1045 (Sov. J. Plasma Phys. **10**, 602).
Sobelman, I. I., Vainshtein, L. A., and Yukov, E. A. (1981). *Excitation of Atoms and Broadening of Spectral Lines* (Springer, Berlin).
Spielman, R. B., Hanson, D. L., Palmer, M. A., Matzen, M. K., Hussey, T. W., and Peek, J. M. (1985a). "Efficient X-ray Production from Ultrafast Gas-Puff Z-Pinches," J. Appl. Phys. **57**, 830.
Spielman, R. B., Matzen, M. K., Palmer, M. A., Rand, P. B., Hussey, T. W., and McDaniel, D. H. (1985b). "Z-Pinch Implosions onto Extremely

Low-Density Foam Cylinders," Appl. Phys. Lett. **47**, 229.
Stallings, C., Nielsen, K., and Schneider, R. (1976). "Multiple-Wire Array Load for High-Power Pulsed Generators," Appl. Phys. Lett. **29**, 404.
Stallings, C., Childers, K., Roth, I., and Schneider, R. (1979). "Imploding Argon Plasma Experiments," Appl. Phys. Lett. **35**, 524.
Stephanakis, S. J., Apruzese, J. P., Burkhalter, P. G., Davis, J., Meger, R. A., McDonald, S. W., Mehlman, G., Ottinger, P. F., and Young, F. C. (1986). "Effect of Pulse Sharpening on Imploding Neon *Z*-Pinch Plasmas," Appl. Phys. Lett. **48**, 829.
Stormberg, H.-P., Murayama, S., and Watanabe, Y. (1987). "Angular distribution of x-ray radiation from optically thick *z*-pinch plasmas," J. Appl. Phys. **62**, 4090.
Striganov, A. R. (1983). "Progress in studying the spectra of atoms and ions and the current level of knowledge about them," Usp. Fiz. Nauk. **139**, 719 (Sov. Phys. Usp. **26**, 373).
Stewart, R. E., Dietrich, D. D., Egan, P. O., Fortner, R. J., and Dukart, R. J. (1987). "Spectroscopic studies of an argon plasma produced in a relativistic electron beam gas puff *z*-pinch," J. Appl. Phys. **61**, 126.
Trubnikov, B. A. (1986). "Particle acceleration and neutron production at the necks of plasma pinches," Fiz. Plazmy **12**, 468 (Sov. J. Plasma Phys. **12**, 271).
Turchi, P. J. and Baker, W. L. (1973). "Generation of high-energy plasmas by electromagnetic implosion," J. Appl. Phys. **44**, 4936.
Vertennikov, V. A., Polukhin, S. N., Semenov, O. G., Sidel'nikov, Yu. V. (1981). "Dynamics of a Vacuum-Arc Micropinch," Fiz. Plazmy **7**, 1199 (Sov. J. Plasma Phys. **7**, 656).
Veretennikov, V. A., Dolgov, A. N., Krokhin, O. N., and Semenov. O. G. (1985a). "Micropinch Structure in a High-Current Discharge," Fiz. Plazmy **11**, 1007 (Sov. J. Plasma Phys. **11**, 587).
Veretennikov, V. A., Polukhin, S. N., and Semenov, O. G. (1985b). "Measurement of Faraday rotation in *z*-pinches," Fiz. Plazmy **11**, 1411 (Sov. J. Plasma Phys. **11**, 814).
Vikhrev, V. V. and Braginskiĭ, S. I. (1980). "Dynamics of the *z*-pinch," in *Voprozy teorii plazmy*, edited by M. A. Leontovich (Atomizdat, Moscow), Vol. 10. Translated in *Reviews of Plasma Physics* (Consultants Bureau, New York, 1986), Vol. 10.
Vikhrev, V. V., Ivanov, V. V., and Koshelev, K. N. (1982). "Formation and Evolution of the Micropinch Region in a Vacuum Spark," Fiz. Plazmy **8**, 1211 (Sov. J. Plasma Phys. **8**, 688).
Vikhrev, V. V. and Ivanov, V. V. (1985). "Propagation of a high-temperature plasma along a *z*-pinch," Sov. Phys. Dokl. **30**, 492.
Vivkhrev, V. V., Ivanov, V. V., and Prut, V. V. (1986). "Dynamics of a *Z*-pinch with radiative loss," Fiz. Plazmy **12**, 328 (Sov. J. Plasma Phys. **12**, 190).
Vikhrev, V. V. (1986). "Mechanism for neutron production in *z*-pinches," Fiz. Plazmy **12**, 454 (Sov. J. Plasma Phys. **12**, 262).
Vinogradov, A. V, Sobelman, I. I., and Yukov, E. A. (1975). "Possibility of constructing a far ultraviolet laser utilizing transitions in multiply charged ions in an inhomogeneous plasma," Kvant. Electron. (Moskow) **2**, 105 (Sov. J. Quantum Electron. **5**, 59).
Waisman, E. M. (1979). "The magnetostatic field of a periodic cylindrical array of perfect conductors of arbitrary *x-y* cross section," J. Appl. Phys. **50**, 23.
Warren, S. W. R., Degnan, J. H., Beason, C. W., Price, D. W., and Snell, M. P. (1987). "High-energy photon spectra from a coaxial gas-puff experiment," J. Appl. Phys. **61**, 2771.
Weinberg, I. N. (1985a). "X-ray lithography and microscopy using a small-scale *z*-pinch device," Ph.D. thesis, UC Irvine, CA.
Weinberg, I. N. and Fisher, A. (1985b). "Elemental Imaging of Biological Specimens Using a *Z* Pinch," Appl. Phys. Lett. **47**, 1116.
Weinberg, I. N. and Fisher, A. (1986). "A small-scale *z*-pinch device as an intense soft x-ray source," Nucl. Instrum. Methods A **242**, 535.
Wessel, F. J., Felber, F. S., Wild, N. C., Rayman, H. U., Fisher, A., and Ruden, E. (1986). "Generation of High Magnetic Fields Using a Gas-Puff *Z* Pinch," Appl. Phys. Lett. **48**, 1119.
Whitney, K. G. and Kepple, P. C. (1982). "Spectrum Diagnostics. The Necessity for Detailed Non-LTE Modeling of X-ray Emission from Dense Plasmas," J. Quant. Spectrosc. Radiat. Transfer **27**, 281.
Winick, I. and Doniach, S., Eds. (1980). *Synchrotron Radiation Research* (Plenum, New York).
Wong, S., Gilman, C., Sincerny, P., and Young, T. (1982). "A Scaling Law for *K*-Line Radiation in the Imploding Argon Gas Puff," in *Proceedings of the 1982 IEEE Plasma Science Conference* (unpublished).
Wong, S., Dukart, R., and Burr, L. (1984). "Imploding Gas Puff on Single Wires," Presented at the 26th Annual Meeting, Plasma Physics Division, American Physical Society (unpublished).
Young, F. C., Stephanakis, S. J., and Scherrer, V. E. (1986). "Filtered x-ray diodes for imploding plasma experiments," Rev. Sci. Instrum. **57**, 2174.
Zakharov, S. M., Ivanenkov, G. V., Kolomenskii, A. A., Pikuz, S. A., and Samokhin, A. I. (1983). "Exploding-Wire Plasma in the Diode of a High Current Accelerator," Fiz. Plazmy **9**, 469 (Sov. J. Plasma Phys. **9**, 271).
Zakharov, S. M., Ivanenkov, G. V., Kolomenskii, A. A., Pikuz, S. A., and Samokhin, A. I. (1984). "Pinch Effect in the Plasma of a Laser Burst in the Diode of a High-Current Accelerator," Fiz. Plazmy **10**, 522 (Sov. J. Plasma Phys. **10**, 303).
Zakharov, S. M., Ivanenkov, G. V., Kolomenskii, A. A., Pikuz, S. A., and Samokhin, A. I. (1987). "Plasma of an exploding multiwire load in the diode of a high-current accelerator," Fiz. Plazmy **13**, 206 (Sov. J. Plasma Phys. **13**, 115).